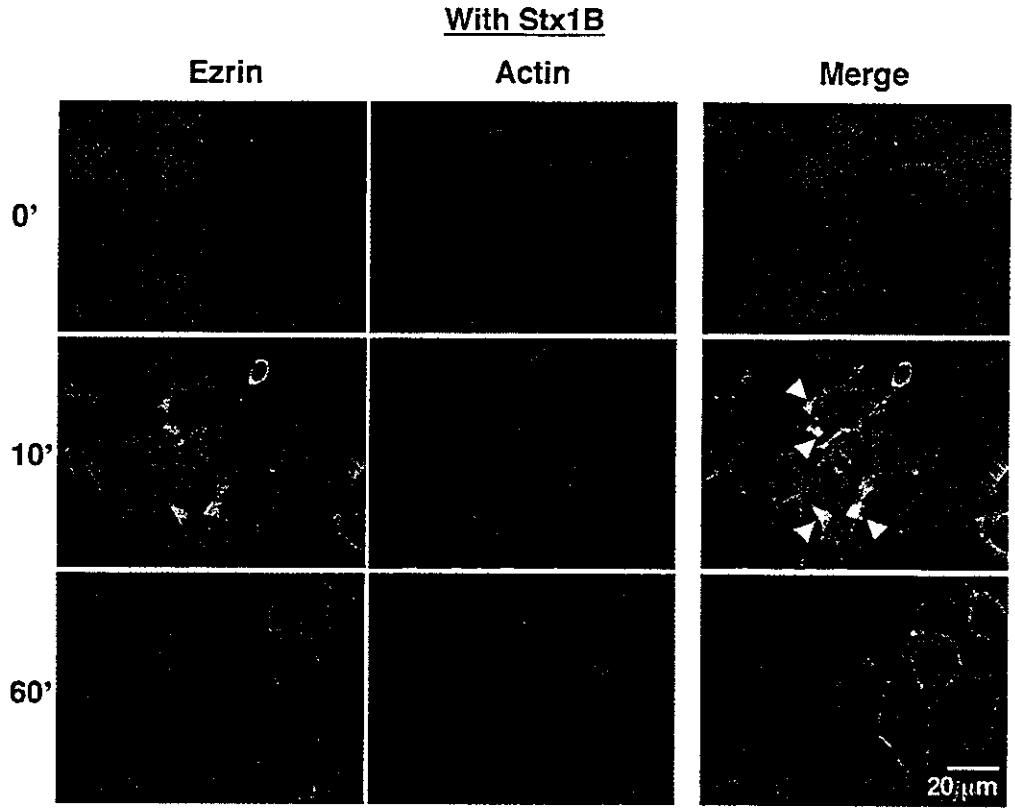

Fig. 2. Effect of Stx1-B subunit on the distribution of ezrin and actin in ACHN cells. ACHN cells treated with the Stx1-B subunit as described in Fig. 1 were double-stained with Alexa-488-labeled anti-ezrin mAb (left panels, green) and TRITC-phalloidin (center panels, red) and visualized using confocal microscopy. The right panels represent the superposition of the green and red images, with DAPI counter staining (blue). The arrowheads indicate the areas of ezrin and actin colocalization (yellow). Results are representative of five independent experiments.

was concentrated in the margin of the cells, as revealed by the brush-like meshwork (Fig. 2, top panels). However, Stx1-B treatment induced a transient enhancement in the concentration of ezrin just beneath the plasma membrane (Fig. 2). Occasionally, the protein clustering peaked at 10 minutes after Stx1-B stimulation (Fig. 2). In parallel, the cortical actin filaments were temporarily polymerized and appeared as thick bundles at the margin of the cells (Fig. 2). The colocalization of both proteins peaked at 10 minutes after Stx1-B stimulation (Fig. 2, yellow area, indicated by arrowhead).

As ERM proteins are thought to play a central role in the organization of cortical actin-based cytoskeletons through the cross-linking of actin filaments and integral membrane, such as CD44 (Tsukita et al., 1994; Tsukita and Yonemura, 1999), we next examined the changes in the distribution of CD44 induced by Stx1-B treatment. As with ezrin, Stx1-B treatment temporarily enhanced the concentration of CD44 in the cell membrane of ACHN cells (Fig. 3). Dual staining with CD44 and F-actin revealed a significant colocalization of both proteins that peaked at 10 minutes after Stx1-B stimulation (Fig. 3, yellow area, indicated by arrowhead).

Paxillin and FAK have been shown to be important for the focal adhesion of cells and growth factor-induced morphological changes (Burridge et al., 1992; Leventhal et al., 1997). Therefore, we examined the effect of Stx1-B stimulation on the distribution of FAK and paxilin. As shown in Fig. 4, most of the FAK and paxillin proteins were independently disseminated throughout the cytoplasm, while small portions of both proteins were colocalized and concentrated within a distinct radial streak at the edges of the cell lamella (yellow area). Upon the addition of Stx1-B, however, the colocalization of FAK and paxillin was temporally enhanced, peaking at 10 minutes after stimulation (Fig. 4, arrowhead).

We further examined the effect of Stx1-B stimulation on other cytoskeletal proteins. The distributions of vimentin and cytokeratin were similar, appearing as a diffuse localization with radial meshwork in the cytoplasm of resting ACHN cells (Fig. 5). Upon Stx1-B stimulation, however, both proteins were temporary concentrated within a paranuclear lesion, peaking at 30 minutes after stimulation in a synchronous manner (Fig. 5, arrowhead).

When the distribution of tubulins was examined using fluorescence immunohistochemistry, a fine mesh work of α-tubulin was seen within the cytoplasm of ACHN cells (Fig. 6). Upon Stx1-B stimulation, the α-tubulin filaments became significantly polymerized, appearing as a thickening of the bundles throughtout the entire cytoplasm and peaking at 10 minutes after stimulation (Fig. 6). Conversely, γ-tubulin was found in cytoplasmic complexes identified as fine spots and specifically concentrated at microtubule-organizing centers (Moritz and Agard, 2001) (Fig. 6). Although the distribution of γ-tubulin did not change significantly after Stx1-B stimulation, a slight enhancement at the microtubule-organizing centers was observed (Fig. 6, arrowhead).

All above observations on Stx1-B-induced cytoskeletal remodeling are entirely based on imaging studies. Therefore, we next examined F-actin formation after Stx1-B stimulation by biochemical means. For this purpose, cell lysate prepared by using actin stabilization buffer was centrifuged and F-actin fraction was separated from soluble G-actin fraction as the pellet. As shown in Fig. 7A, quantification by densitometry of

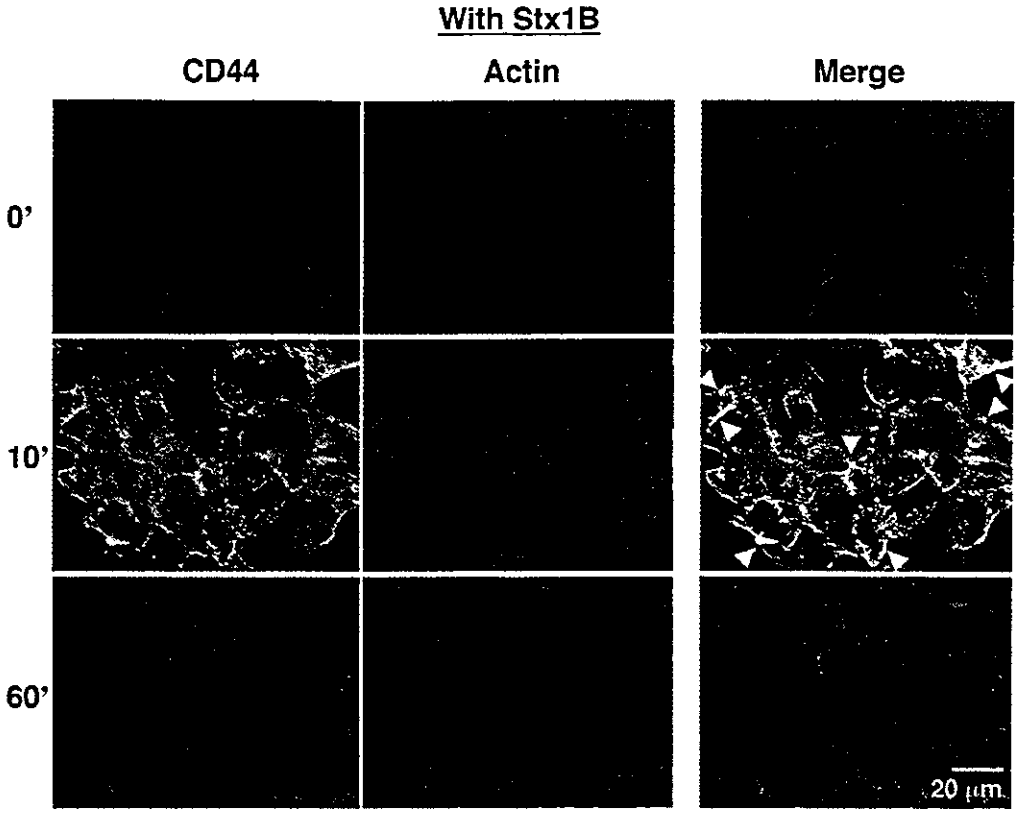

Fig. 3. Effect of Stx1-B subunit on the distribution of CD44 and actin in ACHN cells. ACHN cells were examined as described in Fig. 2 using Alexa-488-labeled anti-CD44 mAb (left panels, green) and TRITC-phalloidin (center panels, red). The arrowheads indicate the areas of CD44 and actin colocalization (yellow). Results are representative of three independent experiments.

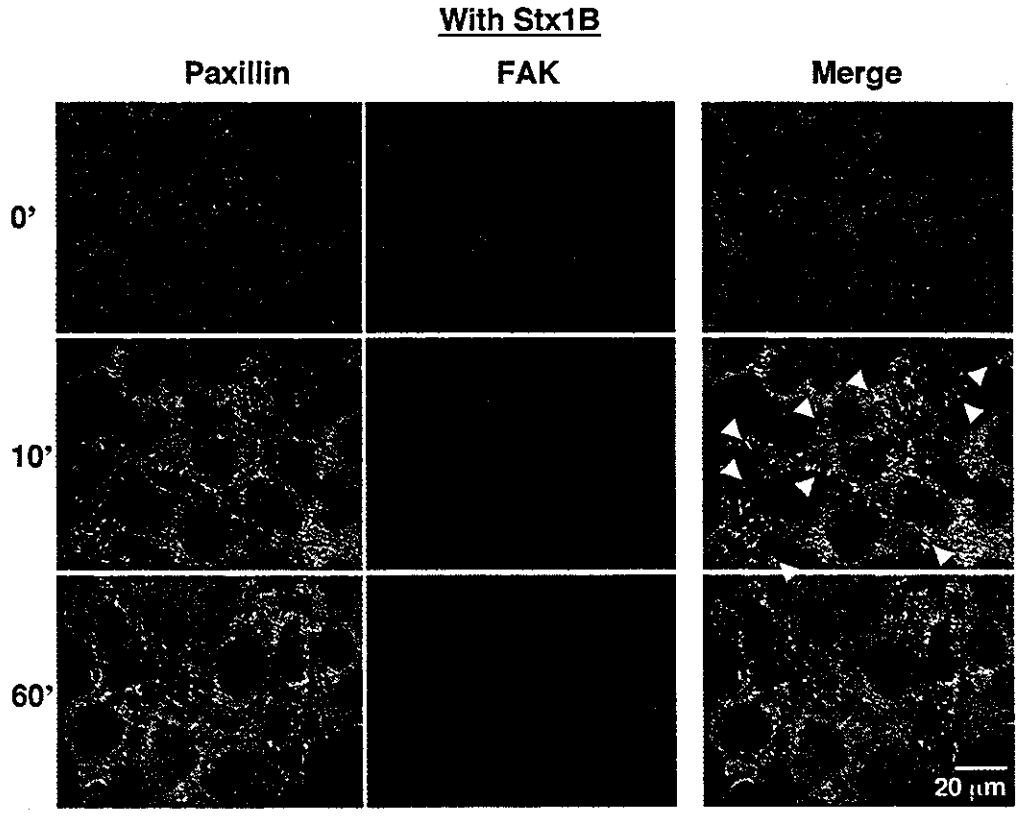

Fig. 4. Effect of Stx1-B subunit on the distribution of paxillin and FAK in ACHN cells. ACHN cells were examined as described in Fig. 2 using Alexa-488-labeled anti-paxillin mAb (left panels, green) and Alexa-546-labeled anti-FAK Ab (center panels, red). The arrowheads indicate the areas of paxillin and FAK colocalization (yellow). Results are representative of three independent experiments.

immunoblots revealed a transient increase in the amount of F-actin fraction, which peaked at 10 to 30 minutes after Stx1-B stimulation. These data coincide with those observed by confocal microscopy experiments using fluorescently labeled phalloidin as a probe for F-actin (Figs 2, 3). We also examined tubulin polymerization similarly. As shown in Fig. 7B, Stx1-

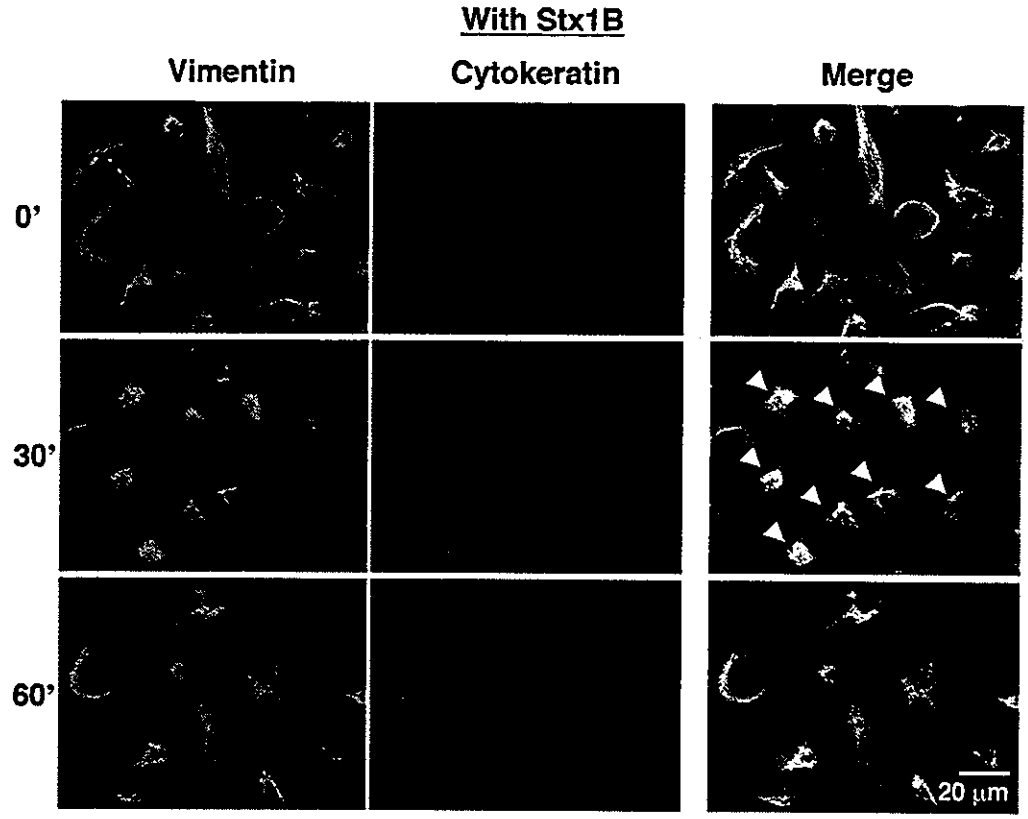

Fig. 5. Effect of Stx1-B subunit on the distribution of vimentin and cytokeratin in ACHN cells. ACHN cells were examined as described in Fig. 2 using Alexa-488-labeled anti-vimentin mAb (left panels, green) and Alexa-546-labeled anti-cytokeratin mAb (center panels, red). The arrowheads indicate the perinuclear clustering of vimentin. Results are representative of three independent experiments.

B-induced transient tubulin polymerization was also confirmed by quantitative analysis.

Stx1-B induces transient phosphorylation of ezrin

The phosphorylation of cytoskeletal proteins plays a key role in cytoskeletal remodeling (Tsukita and Yonemura, 1999). Thus, we attempted to examine whether the phosphorylation state of the cytoskeletal proteins changes. When the total cell lysates prepared from Stx1-B-treated ACHN cells were examined using immunoblotting with Abs that specifically recognize Src family PTKs only when activated by phosphorylation at the C-terminal tyrosine residue, the intensification of three major bands was seen after Stx1-B treatment (Fig. 8A). Based on the molecular weights, the largest band was thought to represent the activated form of Yes, which was previously reported to appear during the course of Stx1-B-mediated activation in ACHN cells (Katagiri et al., 1999; Katagiri et al., 2001). The other smaller bands were thought to represent the activation of other Src family PTK(s) by Stx1-B stimulation. In parallel with the activation of Src family PTKs, the Stx1-B-mediated phosphorylation of both ezrin and paxillin was detected by immunoblotting with Abs that specifically recognize the phosphorylated active forms of ezrin and paxillin (Fig. 8A). The above data indicate that the Stx1-B-mediated intracellular signal induces the phosphorylation of ezrin and paxillin during the course of cytoskeletal remodeling.

As shown in Fig. 8B, the effect of Stx1-B on the induction of ezrin phosphorylation is dose-dependent and the concentration of 1 μg/ml was found to be sufficient to yield maximum effect. As shown in Fig. 8C, we also found that the treatment with anti-Gb3 Abs similarly induces the phosphorylation of ezrin in ACHN cells. Therefore, the ligation of Gb3 by pentameric Stx1-B is not always required to induce cytoskeletal signaling and the binding of monomeric forms of the ligand to Gb3 might be able to induce ezrin phosphorylation.

We also examined whether constitutive Stx1-B treatment is required to induce ezrin phosphorylation. For this purpose, we bound Stx1-B to ACHN cells on ice and then removed excess toxin by washing, before shifting the temperature to 37°C. As shown in Fig. 8D, after the temperature was shifted to 37°C, transient increase in phosphorylation of ezrin was observed by immunoblotting. Although the elevation of ezrin phosphorylation observed in this experiment is slower than that presented in Fig. 8A, it is probably due to the time lag for warming up of the medium to 37°C after the temperature shift. These data indicate that the primary ligation of the plasma membrane Gb3 pool by Stx1-B is sufficient to induce intracellular signal for cytoskeletal rearrangements.

Effect of inhibitors on Stx1-B-induced cytoskeletal remodeling

To clarify the signaling cascade that induces the phosphorylation of ezrin, we examined the effect of a number of inhibitors on Stx1-B-induced ezrin phosphorylation. As shown in Fig. 9, when ACHN cells were pre-treated with PP2, a specific inhibitor for Src family PTK, the Stx1-B-mediated phosphorylation of ezrin was clearly inhibited. Similary, MBD, which is known to disturb the structure of the lipid rafts through the depletion of cholesterol from the cell membrane,

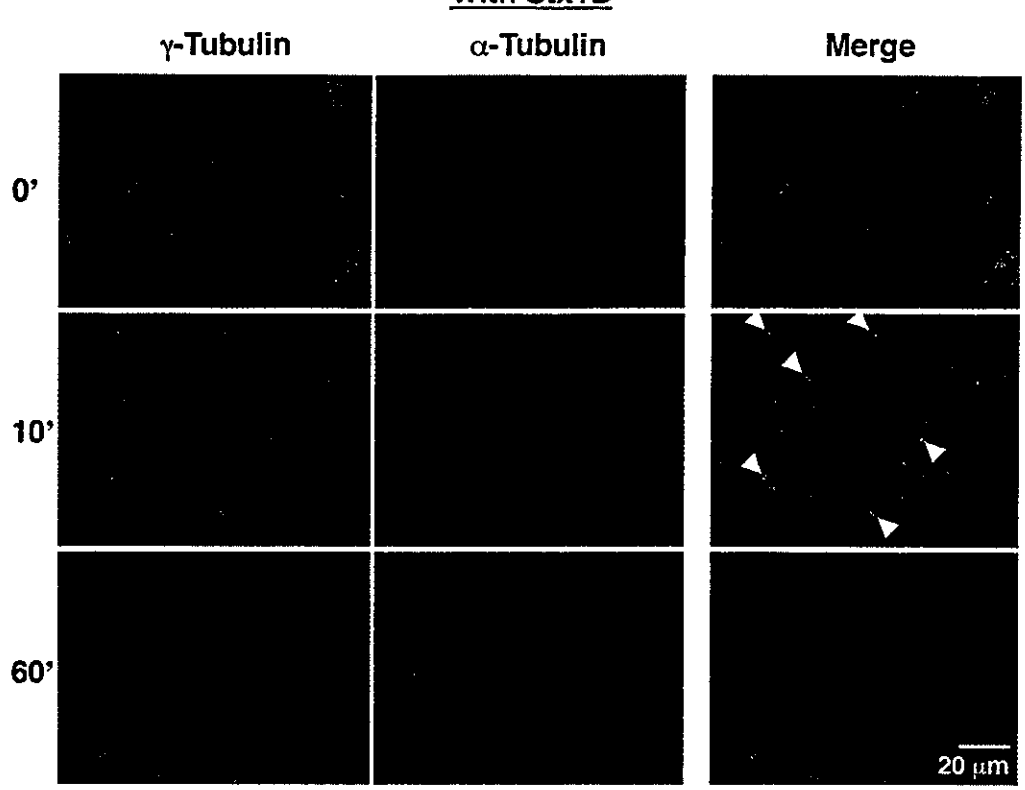

Fig. 6. Effect of Stx1-B subunit on the distribution of γ- and α-tubulins in ACHN cells. ACHN cells were examined as described in Fig. 2 using Alexa-488-labeled anti-γ-tubulin Ab (left panels, green) and Alexa-546-labeled anti-α-tubulin mAb (center panels, red). The arrowheads indicate the accumulation of γ-tubulin at the microtubule-organizing centers. Results are representative of three independent experiments.

inhibited the Stx1-B-mediated phosphorylation of ezrin (Fig. 9). In addition, LY294002, a specific inhibitor for PI3K, and Y27632, a specific inhibitor for ROCK, also inhibited the Stx1-B-mediated phosphorylation of ezrin (Fig. 9). In contrast, PKC inhibitor 20-28 (Fig. 9) and PKC inhibitor EGF-R fragment 651-658 (data not shown) did not affect the Stx1-B-mediated phosphorylation of ezrin in ACHN cells.

We next examined whether these inhibitors affect the Stx1-B-mediated cytoskeletal rearrangements. As shown in Fig. 2 and Fig. 10A, Stx1-B treatment induced the clustering of ezrin beneath the plasma membrane (indicated by arrowhead). When ACHN cells were pretreated with any of inihibitors, including PP2, MBD, LY294002 and Y27632, however, the Stx1-B-induced clustering of ezrin was not observed (Fig. 10A). Therefore, it is suggested that the inhibition of ezrin phosphorylation by these inhibitors suppresses Stx1-B-mediated redistribution of ezrin.

To clarify the molecule responsible for the redistribution of vimentin during the course of Stx1-B-induced cytoskeletal remodeling, we next examined the effect of inhibitors on the Stx1-B-induced redistribution of vimentin. As shown in Fig. 5 and Fig. 10B, Stx1-B treatment induced the accumulation of vimentin in the paranuclear area (indicated by arrowhead). When ACHN cells were pretreated with either PP2 or Y27632, however, the Stx1-B-induced clustering of vimentin in the paranuclear region was not observed (Fig. 10B), indicating the involvement of the Src family PTK and ROCK in the Stx1-B-mediated redistribution of vimentin.

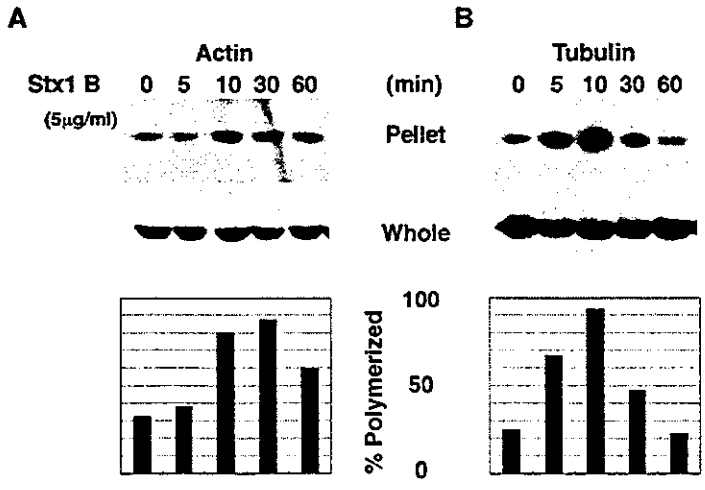

Fig. 7. Effect of Stx1-B subunit on the polymerization of actin and tubulin in ACHN cells. (A) ACHN cells were treated with and without 5 μg/ml of the Stx1-B subunit as described in Fig. 1 and lysed in the actin stabilization buffer. After removing aliquots from each whole lysate for the determination of total actin, polymerized actin (filamentous actin) was separated from soluble actin (monomer actin) by centrifugation. Both fractions of polymerized actin (pellet, upper panel) and total actin (whole, mid panel) were detected by immunoblot analysis and quantitated by densitometry. The proportion (%) polymerized was calculated by dividing the actin in the pellet fraction by the actin in the whole lysate and indicated (lower panel). (B) Tubulin polymerization was examined as in A.

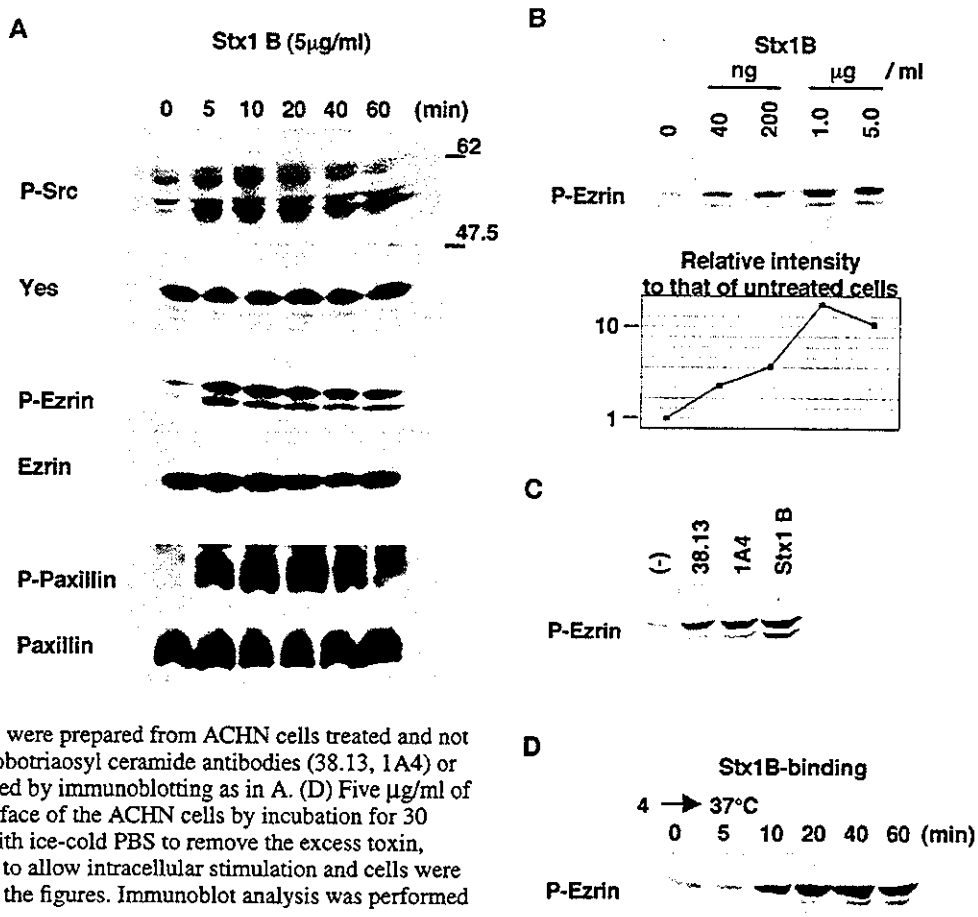

Fig. 8. Transient phosphorylation of ezrin in ACHN cells after treatment with the Stx1-B subunit. (A) Total cell extracts were prepared from ACHN cells treated with or without 5 μg/ml of Stx1-B subunit for the indicated periods. After separation on 10% SDS-PAGE gel, the proteins were transferred to a nitrocellulose membrane and immunoblotted using the indicated antibodies. (B) Total cell extracts were prepared from ACHN cells treated with or without different amounts of Stx1-B subunit for 10 minutes and immunoblot analysis was performed using anti-phospho-specific ezrin antibody (P-Ezrin) as in A. Intensity of the phospho-ezrin signals obtained from each sample was quantitated by densitometry and the relative value of each to that of untreated cells (each value/the value of untreated cells) was indicated as a graph (lower panel). (C) Total cell extracts were prepared from ACHN cells treated and not treated with 5 μg/ml each of either anti-globotriaosyl ceramide antibodies (38.13, 1A4) or Stx1-B subunit for 10 minutes and examined by immunoblotting as in A. (D) Five μg/ml of Stx1-B pentamer was bound to the cell surface of the ACHN cells by incubation for 30 minutes at 4°C. After intensive washing with ice-cold PBS to remove the excess toxin, temperature was shifted from 4°C to 37°C to allow intracellular stimulation and cells were incubated for the time periods indicated in the figures. Immunoblot analysis was performed as in A.

Discussion

In this report, we clearly demonstrated that the binding of Stx1-B induces intracellular signals that initiate cytoskeleton remodeling in ACHN renal carcinoma cells, which are related to renal tubular epithelial cells. These signals led to morphological changes and a weakened adhesiveness of the cells. The series of cellular and biological events induced by Stx1-B binding was similar to that which occurs during the course of growth factor-stimulated cell motility (Bretscher, 1989; Leventhal et al., 1997).

Several lines of evidence, including our own, have suggested that Stx directly injures renal tubular epithelial cells. For example, renal tubular epithelial cells express Gb3, which can bind Stx1 and 2 (Boyd and Lingwood, 1989; Kiyokawa et al., 1998; Taguchi et al., 1998; Uchida et al., 1999). In vitro experiments have revealed that Stx1 induces cell death in renal tubular epithelial cells through protein synthesis inhibition and apoptosis (Karpman et al., 1998; Kiyokawa et al., 1998; Taguchi et al., 1998; Williams et al., 1999). Several clinical studies have indicated the involvement of renal tubular damage during the course of HUS (Kaneko et al., 2001; Takeda et al., 1993). The appearance of apoptotic cells in the renal tubules of the kidney in HUS patients, accompanied by STEC infection, further indicates that renal tubular injury does occur in the kidneys of HUS patients (Karpman et al., 1998; Taguchi et al., 1998).

The essential cytotoxicity of Stx is generally thought to arise from the inhibition of protein synthesis by the Stx-A subunit. However, recent studies have shown that the B-subunit also has biological effects on target cells through a mechanism mediated by intracellular signals upon binding to Gb3 (Katagiri et al., 1999; Kiyokawa et al., 2001; Mangeney et al., 1993; Mori et al., 2000; Taga et al., 1997). Although Stx1-B-induced intracellular signals are known to mediate apoptosis in Burkitt's lymphoma cells, their biological effect on other cell species has not been clarified. The data presented in this study extend previous observations and indicate that Stx1-B-induced intracellular signals induce cytoskeleton remodeling, resulting in morphological changes in the target cells. As previously reported, the simultaneous addition of Stx1-B subunits enhances the cytotoxic effect of Stx1 holotoxins on ACHN cells, suggesting a synergism between A-subunit-mediated protein synthesis inhibition and B-subunit-mediated intracellular signals on the cytotoxicity observed in target cells (Katagiri et al., 2001). Although the biological significance of Stx1-B-induced cytoskeletal remodeling in target cells in vivo is not presently known, this process might participate in Stx-induced cell injury, thereby playing a role in the development of complications associated with STEC infection, such as HUS.

Gb3 acts as functional receptor for Stx, but the natural ligand of this lipid and its normal physiological role are unknown. Upon binding with its natural ligand, Gb3 might mediate intracellular signals leading to cytoskeletal remodeling,

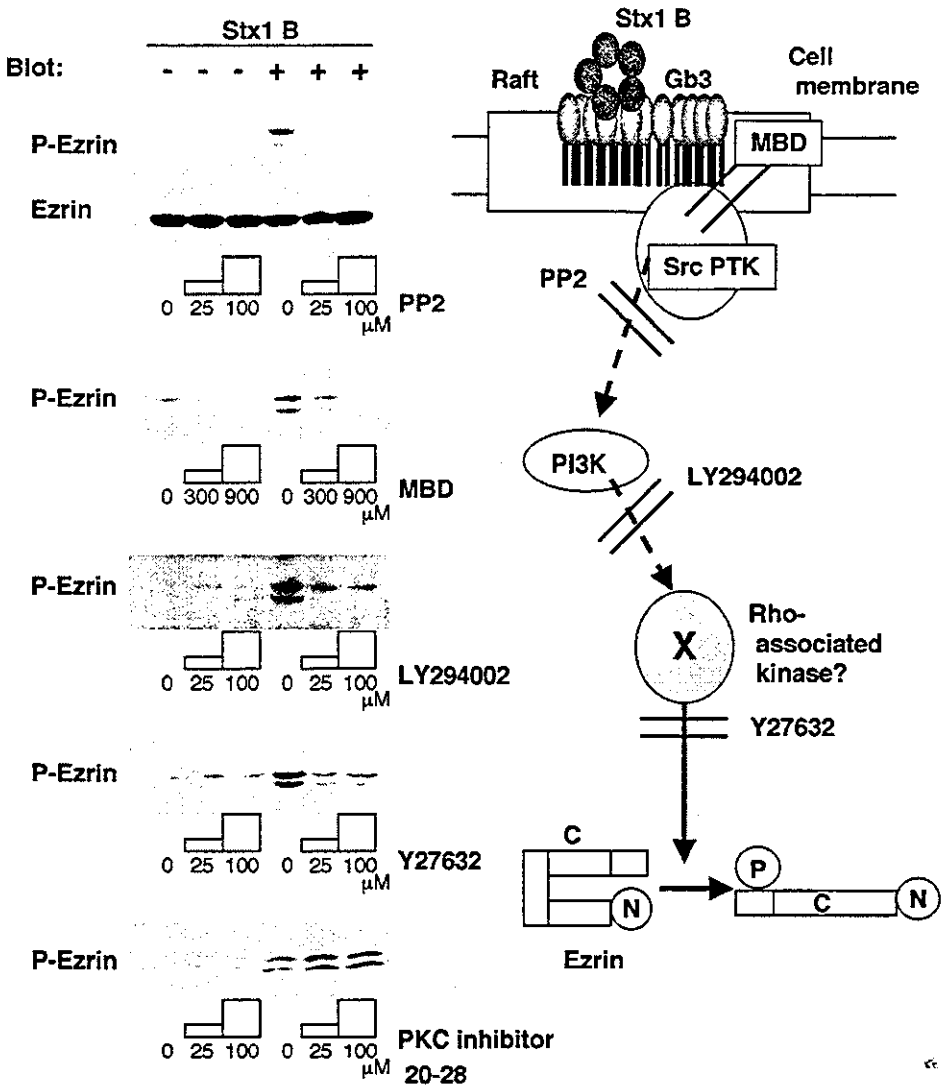

Fig. 9. Effect of inhibitors on the Stx1-B-subunit-mediated phosphorylation of ezrin. ACHN cells were preincubated with the inhibitors shown in the figure for three hours. The concentrations of 300 and 900 μM for MBD and 25 and 100 μM for other inhibitors were used. After treatment with the Stx1-B subunit for 5 minutes, cell extracts were prepared, and immunoblotting for phospho-specific ezrin was performed as described in Fig. 8. In parallel, each sample was examined using an anti-ezrin antibody to confirm that the protein amounts in each lane were comparable (only the result for PP2 is shown in the second panel from the top). In the right panel, the effect of each inhibitor is schematically presented.

participating in the development and organization of kidney tissue. Therefore, our observation might provide an in vitro model for research on lipid-receptor-mediated signaling systems for cytoskeletal remodeling.

Stx1-B binding induces the phosphorylation of ezrin, a linker protein that connects the plasma membrane and the actin cytoskeleton and is involved in cell adhesion and the formation of the free-surface domain of plasma membranes, especially in the ruffling and organization of microvilli (Berryman et al., 1995; Bretscher et al., 1997; Chen et al., 1995; Crepadi et al., 1997; Kondo et al., 1997; Takeuchi et al., 1994; Tsukita and Yonemura, 1999). Stx1-B-induced ezrin phosphorylation was inhibited both by MBD (which disturbs the structure of lipid rafts) and by the Src family PTK inihibitor PP2. Furthermore, we previously reported that Gb3 is mainly located on lipid rafts in the cell membrane, and that Stx1-B binding to Gb3 induces a clustering of the lipid rafts, leading to the activation of Src family PTK (which is anchored to the inner layer of the lipid rafts) possibly by aggregation-mediated kinase auto-phosphorylation (Katagiri et al., 1999; Mori et al., 2000). Thus, our data indicate that the lipid-raft-mediated activation of Src family PTK might play an important role in the phosphorylation of ezrin during the course of Stx-induced cytoskeleton remodeling. In addition to MBD and PP2, we also found that the inhibition of both PI3K and ROCK by their specific inhibitors abolished the Stx1-B-mediated phosphorylation of ezrin, suggesting that these molecules are located downstream from Src family PTK in the signaling cascade and participate in the Stx1-B-mediated phosphorylation of ezrin.

Several molecules have been postulated to be responsible for the phosphorylation of ezrin. For example, the Ras superfamily small G-proteins Rho, Rac and Cdc42 have been shown to be responsible for the formation of focal contact, lamellipodia and filopodia, respectively (Van Aelst and D'Souza-Schorey, 1997; Mackay and Hall, 1998). During these processes, the ERM proteins are thought to be located downstream of the small G-proteins (Bretscher et al., 1997; Matsui et al., 1998; Shaw et al., 1998; Tsukita and Yonemura, 1999). Furthermore, it has been shown that ROCK phosphorylates the C-terminal threonines of ERM proteins, regulating their head-to-tail association in in vitro experiments (Matsui et al., 1998).

We also know that myotonic dystrophy kinase-related Cdc42-binding kinase (MRCK) is a candidate for the kinase that phosphorylates ERM proteins at filopodia (Nakamura et al., 2000). In the case of Merlin, which is closely related to the ERM proteins, p21-activated kinase 2 (PAK2), a downstream effector of Rac and Cdc42, has been postulated as a candidate for the kinase that phosphorylates this protein (Kissil et al., 2002). Consistent with the above observations, we report here that the ROCK inhibitor Y27632 inhibited the Stx1-B-stimulated phosphorylation of ezrin, suggesting that ROCK is at least one of the kinases responsible for ezrin phosphorylation in Stx1-B-induced cytoskeletal remodeling. In addition, Rac and Cdc42 might also be involved in the process, as Stx1-B stimulation induces the extension of lamellipodia- and

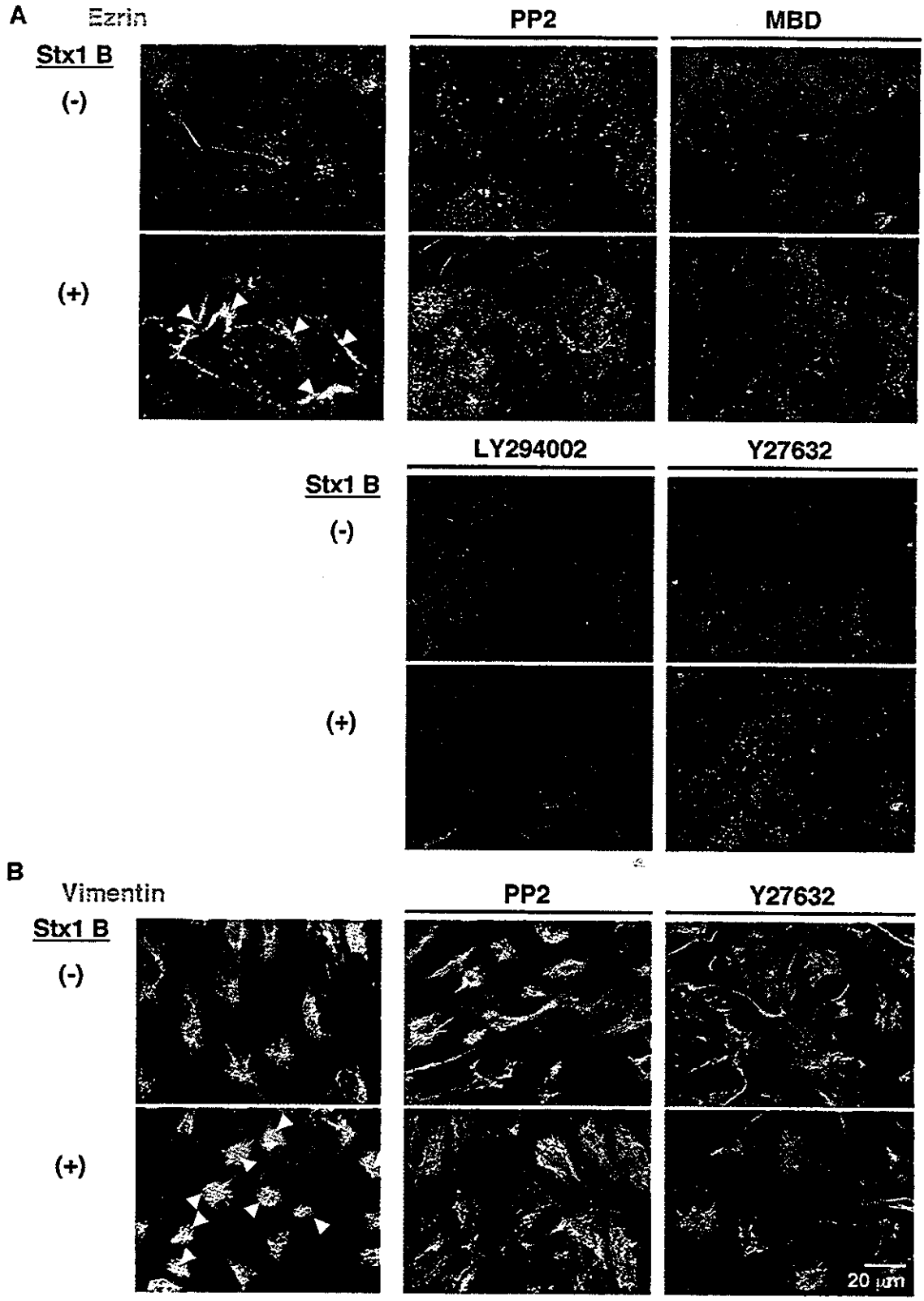

Fig. 10. Effect of inhibitors on the Stx1-B-subunit-mediated clustering of ezrin and vimentin. (A) ACHN cells were preincubated with the inhibitors shown in the figure for three hours. The concentrations of 900 μM for MBD and 100 μM for other inhibitors were used. After treatment with the Stx1-B subunit for 10 minutes, the cells were fixed and stained with anti-ezrin monoclonal antibody (green) followed by counterstaining with DAPI (blue) as in Fig. 2. Results are representative of three independent experiments. The clustering of ezrin was indicated by arrowhead. (B) ACHN cells pre-incubated with inhibitors as in A were treated with the Stx1-B for 30 minutes and stained with anti-vimentin monoclonal antibody (green) as in A.

filopodia-like structures. Further experiments investigating the involvement of small G-proteins and their downstream kinases in the Stx1-B-induced signaling system of cytoskeletal remodeling are now underway.

Conversely, it has been suggested that ezrin was a downstream effector of PKCα during the course of integrin-mediated cell migration (Ng et al., 2001). PKCθ is a major kinase specific for moesin, a family protein of ezrin (Pietromonaco et al., 1998). PKCθ is involved in regulating the localization and association of CD44 and ezrin during cell motility and invasion (Legg et al., 2002; Stapleton et al., 2002). As shown in this study, however, the PKC-inhibitors did not affect the Stx1-B-stimulated phosphorylation of ezrin. Our data might indicate that PKCs are not essential for the Stx1-B-induced phosphorylation of ezrin in our experimental system.

In addition to the phosphorylation of ezrin, we also observed changes in the distributions of several molecules, including FAK, paxillin, vimentin, cytokeratin and tubulins, all of which contribute to the organization of the cytosleleton. The molecular mechanism responsible for the above-described redistribution of cytoskeletal molecules has not yet been clarified. However, as observed in the present study, treatment with the ROCK inhibitor Y27632 abolished the Stx1-B-stimulated relocalization of vimentin, suggesting the involvement of ROCK in the Stx1-B-induced redistribution of vimentin. The ability of ROCK to phosphorylate vimentin in vitro and in vivo (Goto et al., 1998; Kosako et al., 1999) might support this idea.

In conclusion, Stx1-B-induced intracellular signals mediate the remodeling of a variety of cytoskeletal organizing proteins, resulting in changes in cell morphology. Although additional studies are clearly necessary, further investigation of the mechanism of Stx1-B-mediated cytoskeletal remodeling should provide an in vitro model for future research on the pathogenesis of Stx-mediated cell injury as well as the role of lipid raft-mediated cell signaling in cytoskeletal remodeling.

This work was supported in part by Health and Labour Sciences Research Grants from the Ministry of Health, Labour and Welfare of Japan and MEXT. KAKENHI 15019129, JSPS. KAKENHI 15390133 and 15590361. This work was also supported by a grant from the Japan Health Sciences Foundation for Research on Health Sciences Focusing on Drug Innovation. Additional support was provided by a grant from Sankyo Foundation of Life Science. We thank M. Sone and S. Yamauchi for their excellent secretarial works. We thank S. Hakomori and Otsuka Assay Laboratories for gifting anti-Gb3 mAb 1A4.

References

Andreoli, C., Martin, M., le Borgne, R., Reggio, H. and Mangeat, P. (1994). Ezrin has properties to self-associate at the plasma membrane. *J. Cell Sci.* **107**, 2509-2521.

Arpin, M., Algrain, M. and Louvard, D. (1994). Membrane-actin microfilament connections: an increasing diversity of players related to band 4.1. *Curr. Opin. Cell Biol.* **6**, 136-141.

Berryman, M., Gary, R. and Bretscher, A. (1995). Ezrin oligomers are major cytoskeletal components of placental microvilli: a proposal for their involvement in cortical morphogenesis. *J. Cell Biol.* **131**, 1231-1242.

Boyd, B. and Lingwood, C. (1989). Verotoxin receptor glycolipid in human renal tissue. *Nephron* **51**, 207-210.

Bretscher, A. (1989). Rapid phosphorylation and reorganization of ezrin and spectrin accompany morphological changes induced in A-431 cells by epidermal growth factor. *J. Cell Biol.* **108**, 921-930.

Bretscher, A., Gary, R. and Berryman, M. (1995). Soluble ezrin purified from placenta exists as stable monomers and elongated dimers with masked C-terminal ezrin-radixin-moesin association domains. *Biochemistry* **34**, 16830-16837.

Bretscher, A., Reczek, D. and Berryman, M. (1997). Ezrin: a protein requiring conformational activation to link microfilaments to the plasma membrane in the assembly of cell surface structures. *J. Cell Sci.* **110**, 3011-3018.

Burridge, K., Turner, C. E. and Romer, L. H. (1992). Tyrosine phosphorylation of paxillin and pp125FAK accompanies cell adhesion to extracellular matrix: a role in cytoskeletal assembly. *J. Cell Biol.* **119**, 893-903.

Chen, J., Cohn, J. A. and Mandel, L. J. (1995). Dephosphorylation of ezrin as an early event in renal microvillar breakdown and anoxic injury. *Proc. Natl. Acad. Sci. USA* **92**, 7495-7499.

Crepaldi, T., Gautreau, A., Comoglio, P. M., Louvard, D. and Arpin, M. (1997). Ezrin is an effector of hepatocyte growth factor-mediated migration and morphogenesis in epithelial cells. *J. Cell Biol.* **138**, 423-434.

Glogauer, M., Arora, P., Yao, G., Sokholov, I., Ferrier, J. and McCulloch, C. A. (1997). Calcium ions and tyrosine phosphorylation interact coordinately with actin to regulate cytoprotective responses to stretching. *J. Cell Sci.* **110**, 11-21.

Goto, H., Kosako, H., Tanabe, K., Yanagida, M., Sakurai, M., Amano, M., Kaibuchi, K. and Inagaki, M. (1998). Phosphorylation of vimentin by Rho-associated kinase at a unique amino-terminal site that is specifically phosphorylated during cytokinesis. *J. Biol. Chem.* **273**, 11728-11736.

Heacock, C. S. and Bamburg, J. R. (1983). The quantification of G- and F-actin in cultured cells. *Anal. Biochem.* **135**, 22-36.

Heiska, L., Alfthan, K., Gronholm, M., Vilja, P., Vaheri, A. and Carpen, O. (1998). Association of ezrin with intercellular adhesion molecule-1 and -2 (ICAM-1 and ICAM-2). Regulation by phosphatidylinositol 4, 5-bisphosphate. *J. Biol. Chem.* **273**, 21893-21900.

Hirao, M., Sato, N., Kondo, T., Yonemura, S., Monden, M., Sasaki, T., Takai, Y., Tsukita, S. and Tsukita, S. (1996). Regulation mechanism of ERM (ezrin/radixin/moesin) protein/plasma membrane association: possible involvement of phosphatidylinositol turnover and Rho-dependent signaling pathway. *J. Cell Biol.* **135**, 37-51.

Kaneko, K., Kiyokawa, N., Ohtomo, Y., Nagaoka, R., Yamashiro, Y., Taguchi, T., Mori, T., Fujimoto, J. and Takeda, T. (2001). Apoptosis of renal tubular cells in Shiga-toxin-mediated hemolytic uremic syndrome. *Nephron* **87**, 182-185.

Kaplan, B. S., Cleary, T. G. and Obrig, T. G. (1990). Recent advances in understanding the pathogenesis of the hemolytic uremic syndromes. *Pediatr. Nephrol.* **4**, 276-283.

Karpman, D., Hakansson, A., Perez, M. T., Isaksson, C., Carlemalm, E., Caprioli, A. and Svanborg, C. (1998). Apoptosis of renal cortical cells in the hemolytic-uremic syndrome: in vivo and in vitro studies. *Infect. Immun.* **66**, 636-644.

Katagiri, U. Y., Mori, T., Nakajima, H., Katagiri, C., Taguchi, T., Takeda, T., Kiyokawa, N. and Fujimoto, J. (1999). Activation of Src family kinase Yes induced by Shiga toxin binding to globotriaosyl ceramide (Gb3/CD77) in low density, detergent-insoluble microdomains. *J. Biol. Chem.* **274**, 35278-35282.

Katagiri, U. Y., Kiyokawa, N. and Fujimoto, J. (2001). The effect of Shiga toxin binding to globotriaosylceramide in rafts of human kidney cells and Burkitt's lymphomaa cells. *Trends. Glycosci. Glycotech.* **13**, 281-290.

Kissil, J. L., Johnson, K. C., Eckman, M. S. and Jacks, T. (2002). Merlin phosphorylation by p21-activated kinase 2 and effects of phosphorylation on merlin localization. *J. Biol. Chem.* **277**, 10394-10399.

Kiyokawa, N., Taguchi, T., Mori, T., Uchida, H., Sato, N., Takeda, T. and Fujimoto, J. (1998). Induction of apoptosis in normal human renal tubular epithelial cells by *Escherichia coli* Shiga toxins 1 and 2. *J. Infect. Dis.* **178**, 178-184.

Kiyokawa, N., Mori, T., Taguchi, T., Saito, M., Mimori, K., Suzuki, T., Sekino, T., Sato, N., Nakajima, H., Katagiri, Y. U. et al. (2001). Activation of the caspase cascade during Stx1-induced apoptosis in Burkitt's lymphoma cells. *J. Cell. Biochem.* **81**, 128-142.

Knowles, G. C. and McCulloch, C. A. (1992). Simultaneous localization and quantification of relative G and F actin content: optimization of fluorescence labeling methods. *J. Histochem. Cytochem.* **40**, 1605-1612.

Kojio, S., Zhang, H., Ohmura, M., Gondaira, F., Kobayashi, N. and Yamamoto, T. (2000). Caspase-3 activation and apoptosis induction coupled with the retrograde transport of shiga toxin: inhibition by brefeldin A. *FEMS Immunol. Med. Microbiol.* **29**, 275-281.

Kondo, T., Takeuchi, K., Doi, Y., Yonemura, S., Nagata, S. and Tsukita, S. (1997). ERM (ezrin/radixin/moesin)-based molecular mechanism of microvillar breakdown at an early stage of apoptosis. *J. Cell Biol.* **139**, 749-758.

Kosako, H., Goto, H., Yanagida, M., Matsuzawa, K., Fujita, M., Tomono, Y., Okigaki, T., Odai, H., Kaibuchi, K. and Inagaki, M. (1999). Specific accumulation of Rho-associated kinase at the cleavage furrow during cytokinesis: cleavage furrow-specific phosphorylation of intermediate filaments. *Oncogene* **18**, 2783-2788.

Legg, J. W., Lewis, C. A., Parsons, M., Ng, T. and Isacke, C. M. (2002). A novel PKC-regulated mechanism controls CD44 ezrin association and directional cell motility. *Nat. Cell Biol.* **4**, 399-407.

Leventhal, P. S., Shelden, E. A., Kim, B. and Feldman, E. L. (1997). Tyrosine phosphorylation of paxillin and focal adhesion kinase during insulin-like growth factor-I-stimulated lamellipodial advance. *J. Biol. Chem.* **272**, 5214-5218.

Lingwood, C. A. (1996). Role of verotoxin receptors in pathogenesis. *Trends Microbiol.* **4**, 147-153.

Mackay, D. J. and Hall, A. (1998). Rho GTPases. *J. Biol. Chem.* **273**, 20685-20688.

Mangeney, M., Lingwood, C. A., Taga, S., Caillou, B., Tursz, T. and Wiels, J. (1993). Apoptosis induced in Burkitt's lymphoma cells via Gb3/CD77, a glycolipid antigen. *Cancer Res.* **53**, 5314-5319.

Matsui, T., Maeda, M., Doi, Y., Yonemura, S., Amano, M., Kaibuchi, K., Tsukita, S. and Tsukita, S. (1998). Rho-kinase phosphorylates COOH-terminal threonines of ezrin/radixin/moesin (ERM) proteins and regulates their head-to-tail association. *J. Cell Biol.* **140**, 647-657.

McCormack, S. A., Ray, R. M., Blanner, P. M. and Johnson, L. R. (1999). Polyamine depletion alters the relationship of F-actin, G-actin, and thymosin beta4 in migrating IEC-6 cells. *Am. J. Physiol.* **276**, C459-C468.

Minotti, A. M., Barlow, S. B. and Cabral, F. (1991). Resistance to antimitotic drugs in Chinese hamster ovary cells correlates with changes in the level of polymerized tubulin. *J. Biol. Chem.* **266**, 3987-3994.

Montgomery, R. B., Guzman, J., O'Rourke, D. M. and Stahl, W. L. (2000). Expression of oncogenic epidermal growth factor receptor family kinases induces paclitaxel resistance and alters beta-tubulin isotype expression. *J. Biol. Chem.* **275**, 17358-17363.

Mori, T., Kiyokawa, N., Katagiri, Y. U., Taguchi, T., Suzuki, T., Sekino, T., Sato, N., Ohmi, K., Nakajima, H., Takeda, T. et al. (2000). Globotriaosyl ceramide (CD77/Gb3) in the glycolipid-enriched membrane domain participates in B-cell receptor-mediated apoptosis by regulating lyn kinase activity in human B cells. *Exp. Hematol.* **28**, 1260-1268.

Moritz, M. and Agard, D. A. (2001). γ-tubulin complexes and microtubule nucleation. *Curr. Opin. Struct. Biol.* **11**, 174-181.

Nakajima, H., Katagiri, Y. U., Kiyokawa, N., Taguchi, T., Suzuki, T., Sekino, T., Mimori, K., Saito, M., Nakao, H., Takeda, T. et al. (2001). Single-step method for purification of Shiga toxin-1 B subunit using receptor-mediated affinity chromatography by globotriaosylceramide-conjugated octyl sepharose CL-4B. *Protein Expr. Purif.* **22**, 267-275.

Nakamura, N., Oshiro, N., Fukata, Y., Amano, M., Fukata, M., Kuroda, S., Matsuura, Y., Leung, T., Lim, L. and Kaibuchi, K. (2000). Phosphorylation of ERM proteins at filopodia induced by Cdc42. *Gene. Cell.* **5**, 571-581.

Ng, T., Parsons, M., Hughes, W. E., Monypenny, J., Zicha, D., Gautreau, A., Arpin, M., Gschmeissner, S., Verveer, P. J., Bastiaens, P. I. et al. (2001). Ezrin is a downstream effector of trafficking PKC-integrin complexes involved in the control of cell motility. *EMBO J.* **20**, 2723-2741.

Pietromonaco, S. F., Simons, P. C., Altman, A. and Elias, L. (1998). Protein kinase C-theta phosphorylation of moesin in the actin-binding sequence. *J. Biol. Chem.* **273**, 7594-7603.

Richardson, S. E., Karmali, M. A., Becker, L. E. and Smith, C. R. (1988). The histopathology of the hemolytic uremic syndrome associated with verocytotoxin-producing *Escherichia coli* infections. *Hum. Pathol.* **19**, 1102-1108.

Rodgers, W. and Rose, J. K. (1996). Exclusion of CD45 inhibits activity of p56lck associated with glycolipid-enriched membrane domains. *J. Cell Biol.* **135**, 1515-1523.

Serrador, J. M., Alonso-Lebrero, J. L., del Pozo, M. A., Furthmayr, H., Schwartz-Albiez, R., Calvo, J., Lozano, F. and Sanchez-Madrid, F. (1997). Moesin interacts with the cytoplasmic region of intercellular adhesion molecule-3 and is redistributed to the uropod of T lymphocytes during cell polarization. *J. Cell Biol.* **138**, 1409-1423.

Shaw, R. J., Henry, M., Solomon, F. and Jacks, T. (1998). RhoA-dependent phosphorylation and relocalization of ERM proteins into apical membrane/actin protrusions in fibroblasts. *Mol. Biol. Cell* **9**, 403-419.

Simons, K. and Ikonen, E. (1997). Functional rafts in cell membranes. *Nature* **387**, 569-572.

Stapleton, G., Malliri, A. and Ozanne, B. W. (2002). Downregulated AP-1 activity is associated with inhibition of protein-kinase-C-dependent CD44 and ezrin localisation and upregulation of PKC theta in A431 cells. *J. Cell Sci.* **115**, 2713-2724.

Taga, S., Carlier, K., Mishal, Z., Capoulade, C., Mangeney, M., Lecluse, Y., Coulaud, D., Tetaud, C., Pritchard, L. L., Tursz, T. et al. (1997). Intracellular signaling events in CD77-mediated apoptosis of Burkitt's lymphoma cells. *Blood* **90**, 2757-2767.

Taguchi, T., Uchida, H., Kiyokawa, N., Mori, T., Sato, N., Horie, H., Takeda, T. and Fujimoto, J. (1998). Verotoxins induce apoptosis in human renal tubular epithelium derived cells. *Kidney Int.* **53**, 1681-1688.

Takeda, T., Dohi, S., Igarashi, T., Yamanaka, T., Yoshiya, K. and Kobayashi, N. (1993). Impairment by verotoxin of tubular function contributes to the renal damage seen in haemolytic uraemic syndrome. *J. Infect.* **27**, 339-341.

Takeuchi, K., Sato, N., Kasahara, H., Funayama, N., Nagafuchi, A., Yonemura, S., Tsukita, S. and Tsukita, S. (1994). Perturbation of cell adhesion and microvilli formation by antisense oligonucleotides to ERM family members. *J. Cell Biol.* **125**, 1371-1384.

Tsukita, S. and Yonemura, S. (1997). ERM (ezrin/radixin/moesin) family: from cytoskeleton to signal transduction. *Curr. Opin. Cell Biol.* **9**, 70-75.

Tsukita, S. and Yonemura, S. (1999). Cortical actin organization: lessons from ERM (ezrin/radixin/moesin) proteins. *J. Biol. Chem.* **274**, 34507-34510.

Tsukita, S., Oishi, K., Sato, N., Sagara, J., Kawai, A. and Tsukita, S. (1994). ERM family members as molecular linkers between the cell surface glycoprotein CD44 and actin-based cytoskeletons. *J. Cell Biol.* **126**, 391-401.

Tsukita, S., Yonemura, S. and Tsukita, S. (1997). ERM proteins: head-to-tail regulation of actin-plasma membrane interaction. *Trends. Biochem. Sci.* **22**, 53-58.

Turunen, O., Wahlstrom, T. and Vaheri, A. (1994). Ezrin has a COOH-terminal actin-binding site that is conserved in the ezrin protein family. *J. Cell Biol.* **126**, 1445-1453.

Uchida, H., Kiyokawa, N., Horie, H., Fujimoto, J. and Takeda, T. (1999). The detection of Shiga toxins in the kidney of a patient with hemolytic uremic syndrome. *Pediatr. Res.* **45**, 133-137.

Van Aelst, L. and D'Souza-Schorey, C. (1997). Rho GTPases and signaling networks. *Genes. Dev.* **11**, 2295-2322.

Williams, J. M., Lea, N., Lord, J. M., Roberts, L. M., Milford, D. V. and Taylor, C. M. (1997). Comparison of ribosome-inactivating proteins in the induction of apoptosis. *Toxicol. Lett.* **91**, 121-127.

Williams, J. M., Boyd, B., Nutikka, A., Lingwood, C. A., Barnett-Foster, D. E., Milford, D. V. and Taylor, C. M. (1999). A comparison of the effects of verocytotoxin-1 on primary human renal cell cultures. *Toxicol. Lett.* **105**, 47-57.

Yonemura, S., Nagafuchi, A., Sato, N. and Tsukita, S. (1993). Concentration of an integral membrane protein, CD43 (leukosialin, sialophorin), in the cleavage furrow through the interaction of its cytoplasmic domain with actin-based cytoskeletons. *J. Cell Biol.* **120**, 437-449.

Immunology 2004 **112** 575–582 doi:10.1111/j.1365-2567.2004.01918.x

Deficiency of BLNK hampers PLC-γ2 phosphorylation and Ca^{2+} influx induced by the pre-B-cell receptor in human pre-B cells

TOMOKO TAGUCHI,*† NOBUTAKA KIYOKAWA,* HISAMI TAKENOUCH,* JUN MATSUI,* WEI-RAN TANG,* HIDEKI NAKAJIMA,* KYOKO SUZUKI,* YUSUKE SHIOZAWA,* MASAHIRO SAITO,* YOHKO U. KATAGIRI,* TAKAO TAKAHASHI,† HAJIME KARASUYAMA,‡ YOSHINOBU MATSUO,§ HAJIME OKITA,* & JUNICHIRO FUJIMOTO* **Department of Developmental Biology, National Research Institute for Child Health and Development, Setagaya-ku, Tokyo, †Department of Pediatrics, Keio University, School of Medicine, Shinjuku-ku, Tokyo, ‡Department of Immune Regulation, Tokyo Medical and Dental University, Graduate School, Tokyo, and §Fujisaki Cell Center, Hayashibara Biochemical Laboratories Inc, Fujisaki, Okayama, Japan*

SUMMARY

B-cell linker protein (BLNK) is a component of the B-cell receptor (BCR) as well as of the pre-BCR signalling pathway, and BLNK$^{-/-}$ mice have a block in B lymphopoiesis at the pro-B/pre-B cell stage. A recent report described the complete loss or drastic reduction of BLNK expression in approximately 50% of human childhood pre-B acute lymphoblastic leukaemias (ALL), therefore we investigated BLNK expression in human pre-B ALL cell lines. One of the four cell lines tested, HPB-NULL cells, was found to lack BLNK expression, and we used these human pre-B ALL cell lines that express and do not express BLNK to investigate the intracellular signalling events following pre-BCR cross-linking. When pre-BCR was cross-linked with anti-μ heavy-chain antibodies, significant phosphorylation of intracellular molecules, including Syk, Shc, ERK MAP kinase, and AKT, and an activation of Ras were observed without regard to deficiency of BLNK expression, suggesting that BLNK is not required for pre-BCR-mediated activation of MAP kinase and phosphatidyl-inositol 3 (PI3) kinase signalling. By contrast, phospholipase C-γ2 (PLC-γ2) phosphorylation and an increase in intracellular Ca^{2+} level mediated by pre-BCR cross-linking were observed only in the BLNK-expressing cells, indicating that BLNK is essential for PLC-γ2-induced Ca^{2+} influx. Human pre-B cell lines expressing and not expressing BLNK should provide an *in vitro* model for investigation of the role of BLNK in the pre-BCR-mediated signalling mechanism.

Keywords B-cell receptor; B cells; signalling/signal transduction

INTRODUCTION

Signals transduced through antigen receptors play essential roles in B-cell development and fate determination. The B-cell antigen receptor (BCR), which consists of a μ heavy chain (HC), conventional light chain (LC), immunoglobulin α (Igα; CD79a), and Igβ (CD79b), mediates different biological responses in B cells, i.e. proliferation, differentiation, growth arrest, or induction of apoptosis, depending on the differentiation and activation stage of the B cell.[1–3]

In contrast to mature B cells, B-cell progenitors do not possess the complete forms of the BCR, but do express BCR-related components. For example, pro-B cells express the Igα/Igβ heterodimer in association with calnexin,[4] an integral membrane protein, and the surrogate light (SL) chain encoded by the VpreB (CD179a) and λ5 (CD179b) genes.[5,6] These molecules have been found to be competent for transducing differentiation signals for pro-B cells.[4]

In addition, pre-B cells that have successfully accomplished rearrangement of the HC genes start to express a premature form of the antigen receptor, i.e. a pre-B-cell

Received 15 December 2004; revised 21 April 2004; accepted 10 May 2004.

Correspondence: Dr Nobutaka Kiyokawa, Department of Developmental Biology, National Research Institute for Child Health and Development, 3-35-31, Taishido, Setagaya-ku, Tokyo 154–8567, Japan. E-mail: nkiyokawa@nch.go.jp

receptor (pre-BCR) consisting of μ HC, SL chains and the Igα/Igβ heterodimers.[7–9] Several studies have shown the vital importance of pre-BCR as a mediator of pre-B-cell differentiation signals.[10–12] Expression of pre-BCR on the cell surface suppresses further recombination of μ HC genes and induces rearrangement of the conventional LC genes, indicating that signals through pre-BCR facilitate the proliferation of successfully developed pre-B cells.

Although the μ HC does not have any enzymatic activity in its cytoplasmic domain to transduce intracellular signals, the regulatory cascade of molecules is involved in BCR-mediated signalling.[2,3] The stimuli conveyed by antigens through BCR activate a number of BCR-associated cytoplasmic protein tyrosine kinases (PTKs), including the Src-family PTKs, Syk and Brutons tyrosine kinase (BTK).[13,14] These PTKs then phosphorylate numerous intracellular proteins and couple BCR stimulation to intracellular signallings, such as phosphoinositide hydrolysis, protein kinase C activation, and activation of Ras-mitogen-activated protein (MAP) kinase pathways.[2,3] A similar molecular cascade for signal transduction has been postulated for pre-BCR signalling.[4,15]

B-cell linker protein (BLNK), also known as SLP-65, BASH and BCA, is a B-cell adaptor molecule that links the cytoplasmic PTKs with phosphorylation of downstream effector molecules[16–18] and plays a crucial role in the BCR signalling system. Since BLNK does not encode any intrinsic enzymatic activity, its function is to serve as a scaffold for assembling molecular complexes that include enzymes and additional linker proteins. Upon BCR stimulation, BLNK couples activated Syk to phospholipase C-γ (PLC-γ), Vav, Grb2 and NCK.[19] In addition, it binds Btk[20,21] and is required for activation of the transcription factor NF-κB.[22] It has been reported consistently that B cells lacking BLNK fail to elicit Ca^{2+} influx following BCR cross-linking and exhibit attenuated activation of all three families of MAP kinases.[19]

BLNK has also been shown to play important roles in pre-BCR signalling, and BLNK-deficient mice show a partial block at the pre-B cell stage characterized by impaired developmental progression from large cycling $CD43^+$ pro-B cells into small resting $CD43^-$ pre-B cells,[23–26] suggesting an essential role of BLNK in pre-BCR signalling that mediates the growth and differentiation of B-cell precursors.

More importantly, it has been reported that some BLNK-deficient mice spontaneously develop pre-B-cell lymphomas that express large amounts of pre-BCR on their surface.[27,28] Consistent with this, approximately 50% of human childhood pre-B acute lymphoblastic leukaemias (ALL) show complete loss or drastic reduction of BLNK expression.[29] These findings indicate that BLNK functions as a tumour suppressor and that loss of BLNK and the accompanying block in pre-B-cell differentiation is one of the primary causes of pre-B ALL, although the precise mechanism is unknown.

We employed human pre-B cell lines that express and do not express BLNK and examined the intracellular signalling events following pre-BCR cross-linking in an attempt to investigate the role of BLNK in pre-BCR-mediated signalling. In this paper, we report the absence of Ca^{2+} influx following pre-BCR ligation in BLNK-negative human pre-B-cell lines, but not interference with pre-BCR-mediated phosphorylation of intracellular molecules. This suggests that BLNK is essential to Ca^{2+} signalling in human pre-B cells but not to other signalling cascades and it should provide an *in vitro* model for studying the role of BLNK in pre-BCR-mediated signalling.

MATERIALS AND METHODS

Cells and reagents

The human pre-B cell lines, NALM-17, HPB-NULL, P30/OHK[30] and NALM-6[31] were used in this study. The cells were cultured in RPMI-1640 supplemented with 10% fetal calf serum at 37° in a humidified 5% CO_2 atmosphere. The mouse monoclonal antibodies (mAbs) used were; anti-μ (G20-127), anti-κ (G20-193), and anti-λ (JDC-12) from Pharmingen (San Diego, CA); anti-BLNK (2B11), anti-Syk (4D10), and anti PLC-γ2 (B-10), from Santa Cruz Biotechnology (Santa Cruz, CA); anti-extracellular signal-regulated kinase (ERK)-1 (MK12) from Transduction Laboratories (Lexington, KY); anti-phosphotyrosine (PY) (4G10) from Upstate Biotechnology Inc. (Lake Placid, NY); anti-μ (AF6) from Beckman/Coulter Inc. (Westbrook, MA); anti-β actin (ZSA1) from Seikagaku Co. (Tokyo, Japan); and anti-μ (DA4.4) from the American Type Culture Collection (Rockville, MD). Anti-λ5 (HSL11), anti-Vpre-B (HSL96) and anti-conformational pre-BCR (HSL2) were also used.[30] As the negative control for flow cytometric analysis, isotype-matched mouse immunoglobulins, IgG1 (KOPC-31C) and IgG2a (G155-178), from Pharmingen were used. The rabbit polyclonal antibodies used were; F(ab')$_2$ fragment of anti-μ HC from Jackson Laboratory, Inc. (West Grove, PA); anti-PLC-γ1, anti-phospho-ERK, anti-phospho-MAP kinase/ERK kinase (MEK), anti-phospho-PLC-γ1, anti-phospho-PLC-γ2 and anti-phospho-AKT from New England Biolabs, Inc. (Beverly, MA); anti-PLC-γ2 from Pharmingen; and anti-Shc from Transduction Laboratories. The goat polyclonal anti-BTK antibody from Santa Cruz Biotechnology was also used. Secondary antibodies, including fluorescein-conjugated and enzyme-conjugated antibodies, were purchased from Jackson.

Immunofluorescence study

The cells were stained with mAbs and analysed by flow cytometry (EPICS-XL, Coulter) as described previously.[32] Staining of cytoplasmic antigens was performed with CytoStain™ Kits (Pharmingen) according to the manufacturer's protocol.

Immunoblotting and immunoprecipitation

Immunoblotting was performed as described previously.[33] Briefly, cell lysates were prepared by solubilizing the cells in lysis buffer (containing 20 mM Na_2PO_4, pH 7·4, 150 mM NaCl, 1% Triton X-100, 1% aprotinin, 5 mM phenylmethylsulphonyl fluoride, 100 mM NaF and 2 mM Na_3VO_4). After centrifugation, supernatants were obtained and the protein concentration of each cell lysate was

determined with a Bio-Rad protein assay kit (Bio-Rad Laboratories, Hercules, CA). Fifty micrograms of each cell lysate were electrophoretically separated on sodium dodecyl sulphate–polyacrylamide gel and transferred onto a nitrocellulose membrane using a semi-dry transblot system (Bio-Rad). After blocking, the membranes were incubated with the appropriate combination of primary and secondary antibodies as indicated, washed intensively, then examined using the enhanced chemiluminescence reagent system (ECL, Amersham Life Science, Buckinghamshire, UK). The results obtained from a 1-min exposure of the ECL-treated membrane to film are presented.

For the immunoprecipitation, 500 μg of the cell lysates was incubated with 1 μg of antibody and 50 μl of 50% protein-G agarose (Boehringer Mannheim Biochemica, Mannheim, Germany) for 1 hr. After intensive washing, the immunoprecipitates were separated by electrophoresis and analysed as described above.

To measure Ras activation, EZ-Detect™ Ras Activation Kits from PIERCE Biotechnology (Rockford, IL) were used according to the manufacturer's protocol.

Ca^{2+} mobilization assay

Intracellular levels of Ca^{2+} were measured by flow cytometry using Fluo 3-AM (Dojin, Kumamoto, Japan) after pre-BCR cross-linking with anti-μ antibodies. Ten million cells were washed and resuspended in 1 ml of OPTI-MEM containing 0·5% bovine serum albumin, and incubated with 1 mM of Fluo 3-AM for 30 min at 37°. After washing, the cells were resuspended in 10 ml of medium, stimulated by adding different concentrations of rabbit anti-human μ HC antibody as described in Figure 4 and the intracellular calcium concentration was measured by flow cytometry as described previously.[34] Calcium ionophore (ionomycin, Sigma-Aldrich Fine Chemicals, St Louis, MO) was used as the positive control. The data obtained were analysed using WINMDI software (distributed by Dr Joe Trotter) and presented as a kinetics line.

RESULTS

Expression of cell surface pre-BCR and BLNK in human pre-B-cell lines

It has been reported that some pre-B-cell lines express pre-BCR on their cell surface, even if not abundantly.[35] To identify cell lines that express pre-BCR on their cell surface, we tested a series of human pre-B-cell lines for surface expression of μ HC. Flow cytometry showed that all four cell lines tested, i.e. lines NALM-6, HPB-NULL, NALM-17, and P30/OHK, expressed μ HC on their cell surface, and that two of them, NALM-17 and HPB-NULL cells, expressed μ HC on their cell surface more abundantly than the others (Fig. 1a). To investigate the cell surface expression of pre-BCR, we examined reactivity to mAb against SL chains. The mAbs HSL11, HSL96 and HSL2 specifically recognize λ5, VpreB and the conformational epitope of pre-BCR, respectively.[30] When evaluated by flow cytometry, the cell lines stained positive with all three mAbs (Fig. 1a), but not with anti-κ and -λ mAb (data not shown), indicating that the pre-BCR is indeed expressed on the cell surface of some pre-B cell lines. It is noteworthy that although NALM-6 cells clearly reacted with both HSL11 (λ5) and HSL96 (VpreB), they revealed much weaker reactivity with HSL2 (conformational epitope of pre-BCR), for which the precise reason is unknown (Fig. 1a).

Since complete loss or drastic reduction of BLNK expression has also been reported in approximately 50% of childhood precursor-B ALL cases[29] we tested pre-B cell lines for expression of BLNK. Immunoblotting revealed abundant expression of BLNK by NALM-17 cells, whereas no BLNK expression was detectable in HPB-NULL cells (Fig. 1b). The NALM-6 and P30/OHK cells showed an intermediate amount of BLNK expression (Fig. 1b). We also investigated HPB-NULL and NALM-17 cells for intracellular BLNK expression by flow cytometry. When membrane-permeabilized cells were stained with fluorescein-labelled anti-BLNK mAb, clear expression of BLNK was observed only in NALM-17 cells (Fig. 1c), consistent with the results of immunoblotting. In contrast, when tested for expression of other B-cell-related signalling molecules, i.e. BTK, Syk, PLC-γ1 and PLC-γ2, by immunoblotting, all four molecules were comparably expressed in all four pre-B cell lines (Fig. 1b). Based on these findings, we decided to use NALM-17 and HPB-NULL cells in the following experiments as *in vitro* models of BLNK-positive and negative pre-B cells, respectively.

Phosphorylation of intracellular proteins induced by pre-BCR cross-linkage in both BLNK-positive and -negative pre-B cells

Next, we investigated whether cross-linking of pre-BCR with anti-μ antibodies would induce tyrosine phosphorylation of intracellular proteins in pre-B cell lines. Evaluation by immunoblotting with the anti-PY mAb, DA4.4 directed against human μ HC was found to cross-link pre-BCR strongly enough to induce tyrosine phosphorylation of intracellular proteins in HPB-NULL cells (Fig. 2a), but isotype-matched control mouse immunoglobulin did not (data not shown). Phosphorylation of the tyrosine residues peaked at 1–5 min after pre-BCR cross-linking and then decreased to a resting level by 30 min (Fig. 2a). Testing of other antibodies specifically reacting with μ HC, including the other clone of anti-μ HC mAb (AF6 and G20-127) and $F(ab')_2$ fragment of rabbit polyclonal anti-μ HC, yielded identical results (data not shown). Based on the results obtained under various conditions, incubation with 10 μg/ml of anti-μ mAb DA4.4 for 5 min was considered the optimal condition for pre-BCR cross-linking.

Next, immunoprecipitation and immunoblotting were used to identify signal transduction molecules located downstream in the pre-BCR signalling cascade in HPB-NULL cells. When Syk PTK (Fig. 2b) and Shc adapter molecules (Fig. 2c) were immunoprecipitated with specific antibodies, a pre-BCR-mediated increase in tyrosine phosphorylation was observed on anti-PY immunoblotting, and use of phospho-specific antibodies revealed that ERK MAP

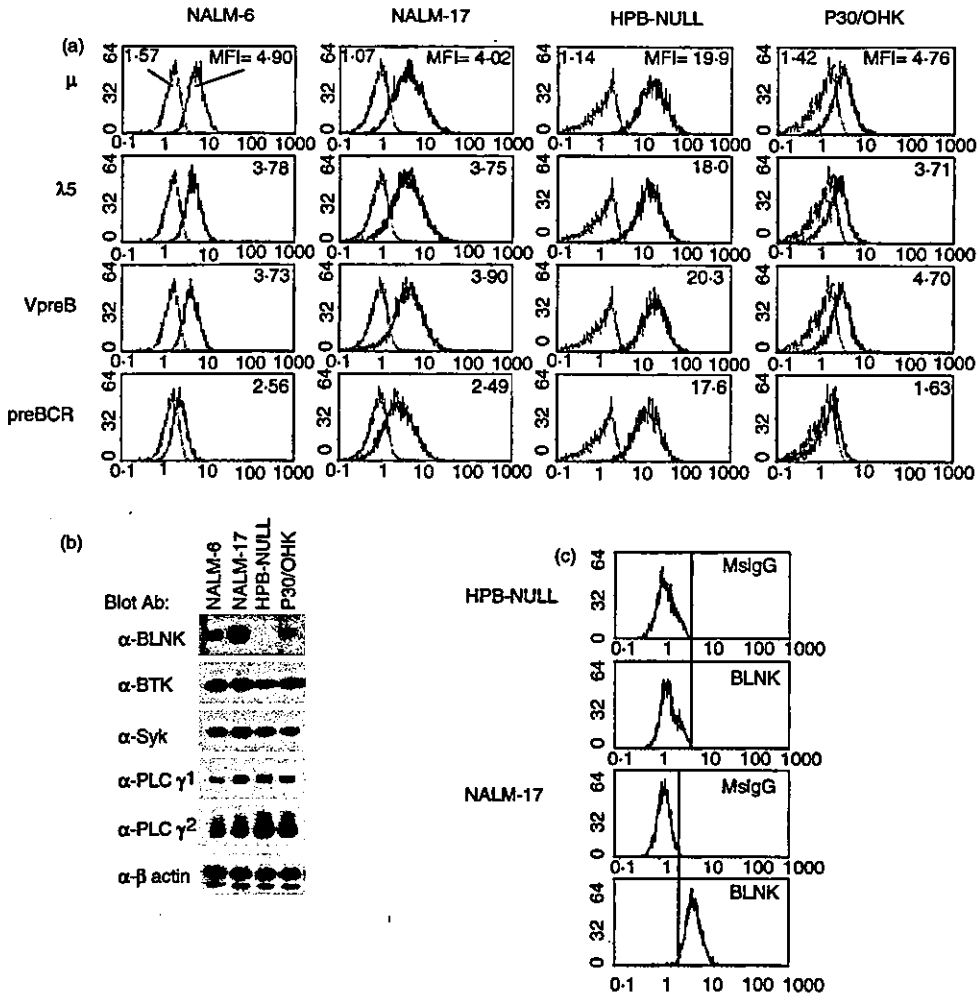

Figure 1. Expression of pre-BCR and BLNK in human pre-B-cell lines. (a) The pre-BCR-related molecules, i.e. μ heavy chain, $\lambda 5$, VpreB and conformational pre-BCR (preBCR), expressed on the cell surface of human pre-B cell lines, NALM-6, NALM-17, HPB-NULL, and P30/OHK, were stained with the specific monoclonal antibodies indicated and analysed by flow cytometry as described in the Materials and methods. The histograms obtained (solid lines) have been superimposed on those of the negative control (cells stained with isotype-matched control mouse immunoglobulin, IgG1 KOPC-31C, light broken lines). The mean fluorescence intensity (MFI) for each staining is presented in the top right hand corner of each panel. The MFI for each negative control staining is presented in the top left hand corner of the top panel of each cell line. The *x*-axis represents fluorescence intensity; the *y*-axis represents relative cell number. (b) Human pre-B-cell lines were tested for expression of BLNK and signal-transduction-related molecules by immunoblotting analysis with the specific antibodies indicated. For PLC-γ2 blotting, anti-PLC-γ2 monoclonal antibody (B-10) was used. (c) Human pre-B cell lines were tested for expression of BLNK by flow cytometry. Cells were permeabilized, stained with a combination of anti-BLNK monoclonal antibody and fluorescein isothiocyanate-conjugated secondary goat anti-mouse IgG, and analysed as described in the Materials and methods. As a negative control, cells were also stained with isotype-matched control mouse immunoglobulin (IgG2a G155-178, MsIgG).

kinase and MEK kinase were phosphorylated immediately after exposure to the anti-μ HC mAb DA4.4 (Fig. 2d). The time course of the phosphorylation state of MEK and MAP kinase showed kinetics similar to those of intracellular proteins detected with anti-PY mAb (Fig. 2a,d), and clear phosphorylation of PLC-γ1 and AKT was also detected in HPB-NULL cells after pre-BCR cross-linking (Fig. 3a). We also examined the activation of Ras, an upstream signalling molecule of ERK MAP kinase. As shown in Fig. 3(b), we observed an activation of Ras in HPB-NULL cells after pre-BCR cross-linking.

Similar testing of BLNK expressing NALM-17 cells revealed that pre-BCR cross-linking induced phosphorylation of these intracellular molecules as well as Ras activation that was as immediate and clear as we observed in HPB-NULL cells (Figs 3a,b). However, it is noteworthy that examination of phosphorylation of PLC-γ2 in the same manner showed that pre-BCR cross-linking induced phosphorylation of PLC-γ2 only in NALM-17 cells, and not in HPB-NULL cells (Fig. 3a).

A major mechanism by which BLNK has been proposed to regulate PLC-γ2 is through the juxtaposition of BTK and

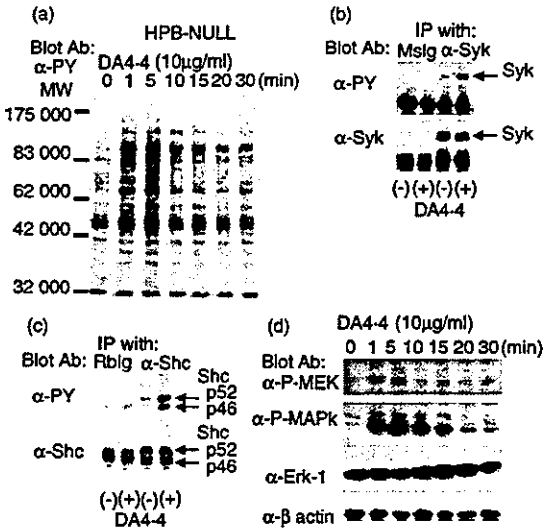

Figure 2. Increase in phosphorylation of intracellular proteins in HPB-NULL cells after exposure to anti-μ antibodies. (a) Immunoblot analysis with anti-phosphotyrosine (α-PY) monoclonal antibody was performed on cell lysates prepared from HPB-NULL pre-B cells exposed to 10 μg/ml of anti-μ mAb DA4.4 for the periods indicated. A molecular weight standard is indicated on the left. (b) Proteins immunoprecipitated with either isotype-matched control mouse immunoglobulin (MsIg, lanes 1 and 2) or mouse monoclonal antibody against Syk (α-Syk, lanes 3 and 4) from HPB-NULL lysates were separated by sodium dodecyl sulphate–polyacrylamide gel electrophoresis in duplicate. After transfer onto a nitrocellulose membrane, the samples were analysed by immunoblotting with either anti-phosphotyrosine (α-PY) monoclonal antibody (upper panel) or anti-Syk monoclonal antibody (lower panel). Corresponding bands for Syk are indicated by arrows. (c) An experiment similar to that in (b) was performed using a combination of HPB-NULL lysates and rabbit polyclonal anti-Shc antibody (α-Shc). (d) The cell lysates prepared from HPB-NULL as in (a) were also tested by immunoblotting with antibodies indicated.

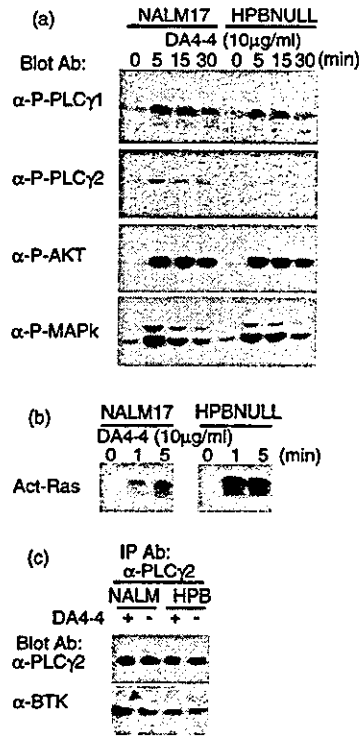

Figure 3. Pre-BCR-mediated signalling in pre-B cell lines. (a) Immunoblot analysis using phospho-specific antibodies on NALM-17 and HPB-NULL cells after exposure to anti-μ monoclonal antibody DA4.4. Cell lysates prepared from NALM-17 and HPB-NULL cells as in Fig. 2(a) were also tested by immunoblotting with the anti-phospho-specific antibodies indicated. (b) NALM-17 and HPB-NULL cells were exposed to DA4.4 and cell lysates were prepared as in (a). Active form of Ras (Ras-GTP) proteins were captured with Raf1-immobilized resin and detected by immunoblotting using anti-Ras antibody. (c) Cell lysates were prepared from NALM-17 and HPB-NULL cells treated with (+) or without (–) DA4.4 (10 μg/ml) for 5 min as in (a). Proteins were immunoprecipitated with rabbit anti-PLC-γ2 antibody from the cell lysates and were separated by SDS–PAGE in duplicate. Immunoblotting was performed with either mouse anti-PLC-γ2 monoclonal antibody (B-10, α-PLC-γ2, upper panel) or goat anti-BTK antibody (lower panel).

PLC-γ2.[3,20,21,28] Therefore we examined the complex formation between BTK and PLC-γ2 in both cell lines. As shown in Fig. 3(c), immunoprecipitation revealed that a portion of BTK was detected in anti-PLC-γ2 immunoprecipitates from the lysates prepared from both NALM-17 and HPB-NULL cells without pre-BCR cross-linking. Interestingly, the total amount of BTK protein precipitated with anti PLC-γ2 antibody was increased after pre-BCR cross-linking in NALM-17 cells, while pre-BCR cross-linking did not affect the amount of BTK protein precipitated with anti PLC-γ2 antibody in HPB-NULL cells (Fig. 3c).

Ca^{2+} influx does not occur in BLNK-negative cell lines after cross-linking of pre-BCR

Next, we investigated whether the cross-linkage of pre-BCR leads to an increase in intracellular Ca^{2+} level. Measurement of the intracellular Ca^{2+} level of HPB-NULL cells by flow cytometry with Fluo 3-AM showed no significant increase in intracellular Ca^{2+} level after exposure to anti-μ antibodies, while treatment with calcium ionophore led to a clear increase in the intracellular Ca^{2+} level (Fig. 4). By contrast, however, when NALM-17 cells, which express BLNK were examined, an increase in intracellular Ca^{2+} level after pre-BCR cross-linkage was observed under identical experimental conditions (Fig. 4). We therefore concluded that the cross-linking of pre-BCR failed to increase intracellular Ca^{2+} in pre-B cells that lack BLNK expression.

DISCUSSION

Several different groups have reported that 5–10% of BLNK-deficient mice spontaneously develop pre-B cell leukaemia/lymphomas expressing large amounts of pre-BCR on their surface.[27,28] Injection of immunodeficient mice with a $BLNK^{-/-}$ pre-B-cell line has been found to result in the development of pre-B-cell leukaemia that was

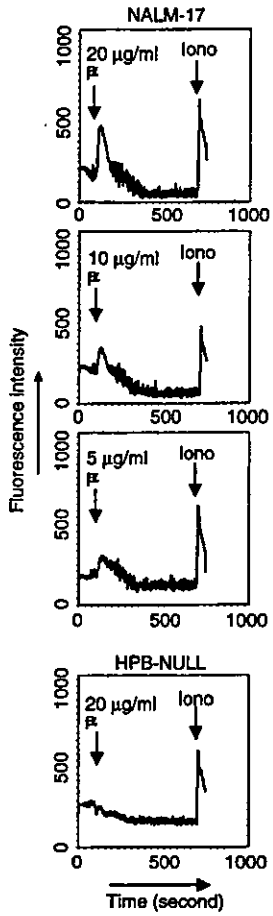

Figure 4. Flow cytometric analysis of Ca^{2+} mobilization in human B-cell lines. NALM-17 or HPB-NULL cells were loaded with Fluo 3-AM as described in the Materials and methods, and the intracellular Ca^{2+} levels were measured by flow cytometry. Rabbit anti-μ monoclonal antibody (α-μ, 5, 10, and 20 μg/ml) or the calcium ionophore ionomycin (Iono, 0·1 μg/ml) was added to the cells at the times indicated by the arrows. Other anti-μ antibodies were also used, and identical results were obtained (data not shown).

prevented by reconstitution of BLNK expression in $BLNK^{-/-}$ pre-B-cell line.[29] More important, it is also reported that 16 of 34 human childhood precursor-B ALL cases showed complete loss or drastic reduction of BLNK expression.[29] Thus, it was hypothesized that BLNK acts as a tumour suppressor and that somatic loss of BLNK and the accompanying block of pre-B-cell differentiation is one of the primary causes of childhood ALL.[27,28] Consistent with the above observations, the results of the present study demonstrated the existence of a human pre-B ALL cell line that lacks BLNK expression, and our findings indicate that the BLNK-deficiency phenotype in human precursor-B ALL cells is maintained in the cell lines established from these ALL cells.

The function of BLNK in pre-B cells is still a matter of controversy. Since, as stated above, reconstitution of BLNK expression in the $BLNK^{-/-}$ pre-B-cell line prevented the development of the leukaemia in immunodeficient mice, Jumaa *et al.* suggested that BLNK is essential to limiting pre-B-cell proliferation.[27,29] By contrast, Hayashi *et al.* observed that the pre-B cells that accumulate in BLNK-deficient mice are mostly non-cycling large pre-B cells, and they therefore concluded that BLNK is critical to pre-BCR signalling that induces proliferation of large pre-B cells.[28] Although the function of BLNK in pre-B ALL cell lines has not yet been clarified, the variable expression levels of BLNK in the pre-B ALL cell lines that we described in this study may mean that the level of expression of BLNK no longer critically affects growth and survival in established human pre-B ALL cell lines. In fact, we did not observe any significant difference in growth rate between the human pre-B ALL cell lines regardless of their BLNK expression level (data not shown).

In the present study we examined the downstream events mediated by cross-linking of pre-BCR in both BLNK-positive and -negative human pre-B-cell lines. The analysis with HPB-NULL cells that lack BLNK clearly indicated that the cross-linking of pre-BCR induces activation of Syk, Shc, Ras, ERK MAP kinase, and AKT, suggesting that the pre-BCR-mediated signalling in the MAP kinase pathway and the phosphatidyl-inositol 3 (PI3) kinase-AKT pathway do not require BLNK. In contrast, cross-linking of pre-BCR induced phosphorylation of PLC-γ2 and an increase in the intracellular Ca^{2+} level in NALM-17 cells alone, and not in HPB-NULL cells, suggesting that BLNK is essential to the pre-BCR-mediated Ca^{2+} influx via PLC-γ2 activation.

Kuwahara *et al.* analysed the downstream events of pre-BCR signalling in the human pre-B cell lines NALM-6 and 796 cells and reported a significant difference in comparison with the events mediated by the conventional BCR expressed on mature B cells, namely, less tyrosine phosphorylation of the cytoplasmic proteins, including Syk, and failure of Ca^{2+} mobilization.[35] However, the fact that the pre-B lines that they studied express only a small amount of pre-BCR on their cell surface may have been a limitation. Thus, their failure to detect signals following pre-BCR cross-linkage may have been because the signals were below the threshold of the detection system.[36] In fact, Nakamura *et al.* analysed the downstream signalling events after pre-BCR stimulation in $\mu\kappa$-transfected NALM-6 cells, which express larger amounts of the reconstituted BCR, and observed that cross-linkage of BCR on pre-B cells caused an elevation in intracellular Ca^{2+} that was qualitatively indistinguishable from the elevation following cross-linkage of BCR on mature B cells.[36]

In addition, we observed that NALM-6 cells clearly reacted with both anti-λ5 and anti-VpreB antibodies, while they revealed much weaker reactivity with antibody against conformational epitope of pre-BCR (Fig. 1a). Although the precise reason for the discrepancy is unknown, our finding may be related to the failure of Ca^{2+} mobilization by pre-BCR cross-linking in NALM-6 cells.

By contrast, our findings also indicated that cross-linkage of pre-BCR expressing on pre-B NALM-17 cells induces hyperphosphorylation of the tyrosine residues in numerous intracellular proteins as well as elevation of the intracellular Ca^{2+} level. Therefore, NALM-17 cells should

provide an *in vitro* model for investigation of the pre-BCR-mediated intracellular signalling mechanism. In addition, since HPB-NULL cells that lack BLNK also revealed similar signalling events induced by pre-BCR cross-linking, with some exceptions such as Ca^{2+} mobilization, comparison between these two cell lines could provide a means of analysing the function of BLNK in human pre-B cells.

BLNK was demonstrated to couple activated Syk to PLC-γ, Vav and Grb2, and participate in the BCR-mediated signalling in mature B cells.[19] Although BLNK has been suggested to also play important roles in pre-BCR signalling, the details remain poorly understood. Based on the molecular similarity of pre-BCR to BCR, however, BLNK is thought to play a role in the pre-BCR signalling system similar to that of BCR, and consistent with this, our results clearly indicated that BLNK is essential for pre-BCR-mediated PLC-γ2 activation and the following Ca^{2+} mobilization. By contrast, they also demonstrated that BLNK is unnecessary for the activation of MAP kinase and the PI3 kinase signalling pathway.

Based on models of transmembrane receptor tyrosine kinases,[37,38] recruitment of the Grb2 adaptor protein, which is associated with Sos GEF, to the plasma membrane was thought to be a likely mechanism for Ras and ERK activation by antigen receptor signalling. However, recent studies have shown that PLC-γ-Ras GRP plays a critical role in Ras activation in the TCR signalling context, in addition to the Grb2-Sos pathway.[39,40] It was also suggested that the latter pathway is dominant in DT40 chicken B cells, because a PLC-γ2-deficient DT40 mutant manifested a large decrease in BCR-mediated ERK activation, whereas it has less of an effect on ERK activation in Grb2-deficient cells, and ablating Sos2, a dominantly expressed Sos isoform in DT40 cells, barely affected ERK activation.[41] As we showed in this study, pre-BCR cross-linking effectively activated Ras and ERK in BLNK-deficient HPB-NULL cells in spite of the impairment of PLC-γ2 phosphorylation and the failure of an increase in complex formation between BTK and PLC-γ2. Thus, our findings may mean that PLC-γ2 activation is unnecessary for the activation of ERK MAP kinase in human pre-B cells. Alternatively, it is also possible that HPB-NULL cells possess a mechanism that partially compensates for the function of BLNK in pre-BCR-mediated signalling, thereby enabling pre-BCR cross-linking to induce ERK activation without PLC-γ2 activation. Interestingly, we observed that PLC-γ1 was expressed and phosphorylated by pre-BCR cross-linking both in BLNK-expressing and BLNK-deficient pre-B-cell lines. The data may indicate that PLC-γ1 and PLC-γ2 have distinct functions in pre-B-cell lines.

As stated above, BLNK-deficient mice have a block in B-cell development at the pre-B-cell stage, but the block is incomplete, and a small number of mature B cells are still present in the periphery.[23–26] This suggests that other signalling molecule(s) may partially neutralize the BLNK deficiency in B cells, and indeed, combined expression of adaptor proteins SLP-76 and LAT has been reported to reconstitute BCR function in $BLNK^{-/-}$ DT40 chicken B cells.[42,43] In addition, most recent reports have suggested that LAT and SLP-76 are involved in pre-BCR signalling and rescue arrested murine $BLNK^{-/-}$ pre-B cells.[44] Thus, alternative signalling molecule(s) that partially compensate for the function of BLNK may be present in HPB-NULL cells.

In conclusion, human pre-B-cell lines NALM-17 and HPB-NULL should provide an ideal *in vitro* model for analysis of pre-BCR-mediated signalling and the role of BLNK in pre-B cells. Further characterization including an analysis on the effect of transfection of the BLNK gene into HPB-NULL cells are clearly necessary. However, experiments using these cell lines will be of assistance in understanding the signalling mechanism in early B-cell development.

ACKNOWLEDGMENTS

We thank M. Sone and S. Yamauchi for their excellent secretarial work. This work was supported in part by Health and Labour Sciences Research Grants from the Ministry of Health, Labour and Welfare of Japan and MEXT. KAKENHI 15019129, JSPS. KAKENHI 15390133 and 15590361. This work was also supported by a grant from the Japan Health Sciences Foundation for Research on Health Sciences Focusing on Drug Innovation. Additional support was provided by a grant from the Sankyo Foundation of Life Science. T. Taguchi is in receipt of a Research Resident Fellowship from the Foundation for Promotion of Cancer Research (Japan) for the 2nd Term Comprehensive 10-Years-Strategy for Cancer Control.

REFERENCES

1 Cambier JC, Pleiman CM, Clark MR. Signal transduction by the B cell antigen receptor and its coreceptors. Annu Rev Immunol 1994; **12**:457–86.
2 Kurosaki T. Genetic analysis of B cell antigen receptor signaling. Annu Rev Immunol 1999; **17**:555–92.
3 Wang LD, Clark MR. B-cell antigen-receptor signalling in lymphocyte development. Immunology 2003; **110**:411–20.
4 Nagata K, Nakamura T, Kitamura F *et al.* The Igα/Igβ heterodimer on m-negative proB cells is competent for transducing signals to induce early B cell differentiation. Immunity 1997; **7**:559–70.
5 Sakaguchi N, Melchers F. λ5, a new light-chain-related locus selectively expressed in pre-B lymphocytes. Nature 1986; **324**:579–82.
6 Kudo A, Melchers F. A second gene, VpreB in the λ5 locus of the mouse, which appears to be selectively expressed in pre-B lymphocytes. EMBO J 1987; **6**:2267–72.
7 Karasuyama H, Kudo A, Melchers F. The proteins encoded by the VpreB and λ5 pre-B cell specific genes can associate with each other and with m heavy chain. J Exp Med 1990; **172**:969–72.
8 Tsubata T, Reth M. The products of pre-B cell-specific genes (λ5 and VpreB) and the immunoglobulin m chain form a complex that is transported onto the cell surface. J Exp Med 1990; **172**:973–6.
9 Lassoued K, Nunez CA, Billips L *et al.* Expression of surrogate light chain receptors is restricted to a late stage in pre-B cell differentiation. Cell 1993; **73**:73–86.
10 Burrows PD, Cooper MD. B-cell development in man. Curr Opin Immunol 1993; **5**:201–6.
11 Melchers F, Rolink A, Grawunder U *et al.* Positive and negative selection events during B lymphopoiesis. Curr Opin Immunol 1995; **7**:214–27.

12 Karasuyama H, Rolink A, Melchers F. Surrogate light chain in B cell development. Adv Immunol 1996; **63**:1–41.
13 Burkhardt AL, Brunswick M, Bolen JB, Mond JJ. Anti-immunoglobulin stimulation of B lymphocytes activates src-related protein-tyrosine kinases. Proc Natl Acad Sci USA 1991; **88**:7410–14.
14 Kurosaki T, Takata M, Yamanashi Y *et al.* Syk activation by the Src-family tyrosine kinase in the B cell receptor signaling. J Exp Med 1994; **179**:1725–9.
15 Guo B, Kato RM, Garcia-Lloret M, Wahl MI, Rawlings DJ. Engagement of the human pre-B cell receptor generates a lipid raft-dependent calcium signaling complex. Immunity 2000; **13**:243–53.
16 Fu C, Turck CW, Kurosaki T, Chan AC. BLNK: a central linker protein in B cell activation. Immunity 1998; **9**:93–103.
17 Wienands J, Schweikert J, Wollscheid B, Jumaa H, Nielsen PJ, Reth M. SLP-65: a new signaling component in B lymphocytes which requires expression of the antigen receptor for phosphorylation. J Exp Med 1998; **188**:791–5.
18 Goitsuka R, Fujimura Y, Mamada H *et al.* BASH, a novel signaling molecule preferentially expressed in B cells of the bursa of Fabricius. J Immunol 1998; **161**:5804–10.
19 Ishiai M, Kurosaki M, Pappu R *et al.* BLNK required for coupling Syk to PLC gamma 2 and Rac1-JNK in B cells. Immunity 1999; **10**:117–25.
20 Hashimoto S, Iwamatsu A, Ishiai M *et al.* Identification of the SH2 domain binding protein of Bruton's tyrosine kinase as BLNK – functional significance of Btk-SH2 domain in B-cell antigen receptor-coupled calcium signaling. Blood 1999; **94**:2357–64.
21 Su YW, Zhang Y, Schweikert J, Koretzky GA, Reth M, Wienands J. Interaction of SLP adaptors with the SH2 domain of Tec family kinases. Eur J Immunol 1999; **29**:3702–11.
22 Tan JE, Wong SC, Gan SK, Xu S, Lam KP. The adaptor protein BLNK is required for b cell antigen receptor-induced activation of nuclear factor-kappa B and cell cycle entry and survival of B lymphocytes. J Biol Chem 2001; **276**:20055–63.
23 Jumaa H, Wollscheid B, Mitterer M, Wienands J, Reth M, Nielsen PJ. Abnormal development and function of B lymphocytes in mice deficient for the signaling adaptor protein SLP-65. Immunity 1999; **11**:547–54.
24 Pappu R, Cheng AM, Li B *et al.* Requirement for B cell linker protein (BLNK) in B cell development. Science 1999; **286**:1949–54.
25 Xu S, Tan JE, Wong EP, Manickam A, Ponniah S, Lam KP. B cell development and activation defects resulting in xid-like immunodeficiency in BLNK/SLP-65-deficient mice. Int Immunol 2000; **12**:397–404.
26 Hayashi K, Nittono R, Okamoto N, Tsuji S, Hara Y, Goitsuka R, Kitamura D. The B cell-restricted adaptor BASH is required for normal development and antigen receptor-mediated activation of B cells. Proc Natl Acad Sci USA 2000; **97**:2755–60.
27 Flemming A, Brummer T, Reth M, Jumaa H. The adaptor protein SLP-65 acts as a tumor suppressor that limits pre-B cell expansion. Nat Immunol 2003; **4**:38–43.
28 Hayashi K, Yamamoto M, Nojima T, Goitsuka R, Kitamura D. Distinct signaling requirements for Dmu selection, IgH allelic exclusion, pre-B cell transition, and tumor suppression in B cell progenitors. Immunity 2003; **18**:825–36.
29 Jumaa H, Bossaller L, Portugal K *et al.* Deficiency of the adaptor SLP-65 in pre-B-cell acute lymphoblastic leukaemia. Nature 2003; **423**:452–6.
30 Tsuganezawa K, Kiyokawa N, Matsuo Y *et al.* Flow cytometric diagnosis of the cell lineage and developmental stage of acute lymphoblastic leukemia by novel monoclonal antibodies specific to human preB cell receptor. Blood 1998; **92**:4317–24.
31 Hurwitz R, Hozier J, LeBien T *et al.* Characterization of a leukemic cell line of the pre-B phenotype. Int J Cancer 1979; **23**:174–80.
32 Kiyokawa N, Kokai Y, Ishimoto K, Fujita H, Fujimoto J, Hata J. Characterization of the common acute lymphoblastic leukemia antigen (CD10) as an activation molecule on mature human B cells. Clin Exp Immunol 1990; **79**:322–7.
33 Kiyokawa N, Lee EK, Karunagaran D, Lin S-Y, Hung M-C. Mitosis-specific negative regulation of epidermal growth factor receptor, triggered by a decrease in ligand binding and dimerization, can be overcome by overexpression of receptor. J Biol Chem 1997; **272**:18656–65.
34 Kabak S, Skaggs BJ, Gold MR *et al.* The direct recruitment of BLNK to immunoglobulin alpha couples the B-cell antigen receptor to distal signaling pathways. Mol Cell Biol 2002; **22**:2524–35.
35 Kuwahara K, Kawai T, Mitsuyoshi S *et al.* Cross-linking of B cell antigen receptor-related structure of pre-B cell lines induces tyrosine phosphorylation of p85 and p110 subunits and activation of phosphatidylinositol 3-kinase. Int Immunol 1996; **8**:1273–85.
36 Nakamura T, Koyama M, Yoneyama A *et al.* Signal transduction through mu kappa B-cell receptors expressed on pre-B cells is different from that through B-cell receptors on mature B cells. Immunology 1996; **88**:593–9.
37 Pawson T, Scott JD. Signaling through scaffold, anchoring, and adaptor proteins. Science 1997; **278**:2075–80.
38 Schlessinger J. Cell signaling by receptor tyrosine kinases. Cell 2000; **103**:211–25.
39 Dower NA, Stang SL, Bottorff DA *et al.* RasGRP is essential for mouse thymocyte differentiation and TCR signaling. Nat Immunol 2000; **1**:317–21.
40 Ebinu JO, Stang SL, Teixeira C *et al.* RasGRP links T-cell receptor signaling to Ras. Blood 2000; **95**:3199–203.
41 Hashimoto A, Okada H, Jiang A *et al.* Involvement of guanosine triphosphatases and phospholipase C-gamma2 in extracellular signal-regulated kinase, c-Jun NH2-terminal kinase, and p38 mitogen-activated protein kinase activation by the B cell antigen receptor. J Exp Med 1998; **188**:1287–95.
42 Ishiai M, Kurosaki M, Inabe K, Chan AC, Sugamura K, Kurosaki T. Involvement of LAT, Gads, and Grb2 in compartmentation of SLP-76 to the plasma membrane. J Exp Med 2000; **192**:847–56.
43 Wong J, Ishiai M, Kurosaki T, Chan AC. Functional complementation of BLNK by SLP-76 and LAT linker proteins. J Biol Chem 2000; **275**:33116–22.
44 Su YW, Jumaa H. LAT links the pre-BCR to calcium signaling. Immunity 2003; **19**:295–305.

Modern Pathology (2004) 17, 423–429
 0893-3952/04 $25.00
www.modernpathology.org

Diagnostic importance of CD179a/b as markers of precursor B-cell lymphoblastic lymphoma

Nobutaka Kiyokawa[1], Takaomi Sekino[1], Tsubasa Matsui[1], Hisami Takenouchi[1], Kenichi Mimori[1], Wei-ran Tang[1], Jun Matsui[1], Tomoko Taguchi[1], Yohko U Katagiri[1], Hajime Okita[1], Yoshinobu Matsuo[2], Hajime Karasuyama[3] and Junichiro Fujimoto[1]

[1]*Department of Developmental Biology, National Research Institute for Child Health and Development, Japan;* [2]*Fujisaki Cell Center, Hayashibara Biochemical Labs Inc, Okayama, Japan and* [3]*Department of Immune Regulation, Tokyo Medical and Dental University, Graduate School of Medicine, Tokyo, Japan*

Surrogate light chains consisting of VpreB (CD179a) and λ5 (CD179b) are expressed in precursor B cells lacking a complete form of immunoglobulin and are thought to act as substitutes for conventional light chains. Upon differentiation to immature and mature B cells, CD179a/b disappear and are replaced with conventional light chains. Thus, these molecules may be useful as essential markers of precursor B cells. To examine the expression of the surrogate light-chain components CD179a and CD179b in precursor B-cell lymphoblastic lymphoma, we analyzed tissue sections using immunohistochemistry techniques. Among a number of monoclonal antibodies for the surrogate light chains, VpreB8 and SL11 were found to detect CD179a and CD179b, respectively, in acetone-fixed fresh frozen sections. Moreover, we also observed VpreB8 staining in formalin-fixed, paraffin-embedded sections. Using these antibodies, we found that CD179a/b were specifically expressed in precursor B-cell lymphoblastic lymphomas, but not in mature B-cell lymphomas in childhood. Furthermore, other pediatric tumors that must be included in a differential diagnosis of precursor B-cell lymphoblastic lymphoma, including precursor T-cell lymphoblastic lymphoma, extramedullary myeloid tumors, and Ewing sarcoma, were also negative for both CD179a and CD179b. Our data indicate that CD179a and CD179b may be important markers for the immunophenotypic diagnosis of precursor B-cell lymphoblastic lymphomas.
Modern Pathology (2004) **17**, 423–429, advance online publication, 20 February 2004; doi:10.1038/modpathol.3800079

Keywords: CD179a/b; lymphoblastic lymphoma; precursor B cells; immunohistochemistry; diagnosis

B cells are characterized by the surface expression of immunoglobulin (Ig), consisting of a heavy chain (HC) and conventional κ or λ light chains (LCs). The Ig expressed in B cells is associated with the Igα/Igβ (CD79a/b) complex and forms a B-cell antigen receptor complex. In contrast to these mature B cells, precursor B cells do not express Ig, although they do contain Ig-related components. For example, more primitive pro-B cells already express the Igα/Igβ complex and contain surrogate LCs, consisting of VpreB (CD179a) and λ5 (CD179b).[1–5] Through the successful rearrangement of HC genes, pro-B cells undergo differentiation into pre-B cells and start to express a premature antigen receptor, namely the pre-B-cell receptor (pre-BCR), consisting of μ HC, CD179a/b and the Igα/Igβ heterodimer.[6–9] Upon further differentiation from pre-B cells to B cells, CD179a/b disappear and are replaced with conventional LC.

The stage-specific developmental expression of Ig-related molecules is an essential characteristic of B-lineage cells and is conserved not only in normal cells but also in neoplastic cells of B lineage. Indeed, precursor B acute lymphoblastic leukemias (ALL), which originate from precursor B cells and lack the complete form of Ig, are known to express CD179a/b, while mature and Ig-expressing B-cell ALLs do not.[10] Precursor B-cell lymphoblastic lymphoma (B-LBL) is a disease in which neoplastic precursor B cells proliferate without the obvious involvement of blood or bone marrow and thus exhibits immunophenotypic characteristics that are similar to those of precursor B-ALL.[11,12] Neoplasms of precursor B cells most commonly present as a form of ALL during childhood, and the presentation of B-LBL is infrequent, but may occur in patients of any

Correspondence: N Kiyokawa, MD, PhD, Department of Developmental Biology, National Research Institute for Child Health and Development, 3-35-31, Taishido, Setagaya-ku, Tokyo 154-8567, Japan.
E-mail: nkiyokawa@nch.go.jp
Received 21 August 2003; revised 26 November 2003; accepted 26 December 2003; published online 20 February 2004

age, frequently involving the skin, bone, or lymph nodes. Owing to the rareness of B-LBL and its morphological and immunophenotypic similarities to mature B-cell lymphomas in some cases, distinguishing between these diseases is of great importance, especially in the field of pediatric oncology, because the treatment strategies for these two diseases are quite different. In addition, other tumors, including precursor T-cell lymphoblastic lymphoma (T-LBL), extramedullary myeloid tumors, and Ewing sarcoma, must also be included in a differential diagnosis of B-LBL.

In an attempt to characterize B-LBL using the expression of Ig-related molecules and to examine the utility of such a method for diagnosis, we examined CD179a/b expression in B-LBL tissues using immunohistochemistry. CD179a/b was found to be specifically expressed in B-LBL, but not in mature B-cell lymphomas and other tumors in childhood. The usefulness of CD179a/b as diagnostic markers for B-LBL is discussed.

Materials and methods

Materials

The human pre-B-cell line HPB-NULL[10] and the Burkitt cell line Ramos (Japanese Cancer Research Resources Bank, Tokyo, Japan) were used in this study. Cells were maintained in RPMI1640 supplemented with 10% fetal calf serum at 37°C in a humidified 5% CO_2 atmosphere.

Biopsy specimens from pediatric patients, including 11 patients with B-LBL, seven patients with Burkitt lymphoma, three patients with diffuse large B-cell lymphoma, seven patients with T-LBL, three patients with extramedullary myeloid tumors, and three patients with Ewing sarcoma, were selected from medical files collected between 1985 and 2003 at the Department of Developmental Biology, National Research Institute for Child Health and Development. In each case, the initial diagnosis was based on morphological observations of hematoxylin and eosin (H&E)-stained, formalin-fixed, paraffin-embedded tissues, the immunophenotypic characteristics revealed by immunohistochemistry using acetone-fixed, fresh frozen sections, and the patient's clinical features. In some cases, immunophenotyping was also performed using flow cytometric analysis of a single-cell suspension prepared from the tissue. To examine CD179a/b expression, snap-frozen tissues in OCT compounds stored at −85°C after the initial diagnosis were used.

The following mouse monoclonal antibodies (mAbs) were used in this study: anti-CD179a (HSL96), anti-CD179b (HSL11), anti-conformational pre-BCR (HSL2),[10] anti-CD20 (L26),[13] anti-HLA-DR,[14] and anti-CD10 (IF6).[15] HSL2 is a unique mAb that does not bind to each component of the pre-BCR, but recognizes a conformational epitope formed only when the μ HC and CD179a/b surrogate LC associate with each other to make the pre-BCR complex.[10] In addition, several commercially available mAbs were also used: anti-μ (G20-127), anti-CD179a (VpreB8 and VpreB9), and anti-CD19 (Leu12) from BD Pharmingen (San Diego, CA, USA); anti-κ (HP6053) and anti-λ (HP6054) from Zymed Laboratories Inc. (San Francisco, CA, USA); anti-CD79a (HM-57), anti-CD22 (4KB128), and anti-TdT (HT-1/3/4) from DAKO (Glostrup, Denmark); anti-CD179a (4G7) from Coulter/Immunotech Inc. (Westbrook, MA, USA); anti-TdT (SEN28) from Nichirei Co. (Tokyo, Japan); and anti-CD179a (B-MAD-688) from Biocarta (San Diego, CA, USA). The anti-CD77 (1A4) used in this study was a generous gift from Dr S Hakomori of the University of Washington, Seattle, WA, USA and Otsuka Assay Laboratories, Kawauchi-cho, Tokushima, Japan. Secondary Abs, including fluorescence- and enzyme-conjugated Abs, were purchased from Jackson Laboratory, Inc., West Grove, PA, USA.

Flow Cytometry

The cells were stained with mAbs and analyzed by flow cytometry (EPICS-XL, Coulter) as described previously.[15] Cytoplasmic antigens were stained using CytoStain™ Kits (BD Pharmingen), according to the manufacturer's protocol.

Immunohistochemistry

Immunohistochemical staining of acetone-fixed fresh frozen sections was performed as described elsewhere.[16] Briefly, fresh frozen sections from each tissue were prepared using a cryostat apparatus and fixed in acetone for 15 min at 4°C. After washing in phosphate-buffered saline (PBS) and blocking with normal rabbit serum, the sections were incubated with mAbs at appropriate dilutions for 30 min at room temperature. Sections were then washed with PBS and incubated with horseradish peroxidase (HRP)-conjugated rabbit anti-mouse antibodies for 30 min at room temperature. After washing with PBS, color development was performed in diaminobenzidine solution (10 mM in 0.05 M Tris-HCl, pH 7.5) with 0.003% H_2O_2.

For the cell line samples, the cells were cytocentrifuged on slide glasses using Cytospin III (Shandon Scientific Ltd., Pittsburgh, PA, USA). After fixation with acetone, immunohistochemical staining was performed as described above. In addition, other fixatives, including paraformaldehyde and Zamboni's fixative, were also tested.

The formalin-fixed, paraffin-embedded tissue specimens were initially deparaffinized and then treated using the heat-induced epitope retrieval method in 10 mM of citrate buffer, pH 6.0; immunohistochemical staining was performed using the CSA system (DAKO) according to the manufacturer's protocol.

Results

Immunohistochemical Staining of CD179a/b in Acetone-fixed Cytocentrifuged Cell Lines

As reported previously and presented in Figure 1, the mAbs HSL96, HSL11, and HSL2 recognized CD179a/VpreB, CD179b/λ5, and conformational pre-BCR, respectively, in membrane-permeabilized cells when analyzed using flow cytometry.[10] We first examined whether these mAbs could also be used for immunohistochemical staining in acetone-fixed cells. When acetone-fixed, cytocentrifuged pre-B-ALL HPB-NULL cells expressing conformational pre-BCR were tested, the HSL11 mAb was able to detect CD179b at a concentration of 5 μg/ml; neither the HSL96 nor the HSL2 mAbs detected this molecule (Figure 1). Typically, a cytoplasmic staining pattern was observed in HPB-NULL cells using HSL11. In contrast, HSL11 did not react with similarly treated Ramos Burkitt cells, which express the complete form of Ig (μλ), but lack the surrogate LCs, suggesting that CD179b binds specifically to SL11.

We also examined the staining patterns produced by commercially available anti-CD179a mAbs: VpreB8, VpreB9, 4G7, and B-MAD-688. When these four anti-CD179a mAbs were examined, only the VpreB8 mAb reacted with CD179a in acetone-fixed HPB-NULL cells (data not shown). However, VpreB8 mAb exhibited a weak nonspecific binding with the nuclei of acetone-fixed Ramos cells at high mAb concentrations. A concentration of 1.25 μg/ml was optimized as a sufficient and specific condition for CD179a detection in precursor B-ALL cells, which does not produce a nonspecific reaction in Burkitt cells (data not shown).

We further examined whether SL11 and VpreB8 could be used for immunohistochemical staining in cells treated with other fixatives and observed that both mAbs react with Zamboni's fixative-treated cells, but not with paraformaldehyde-treated cells (data not shown).

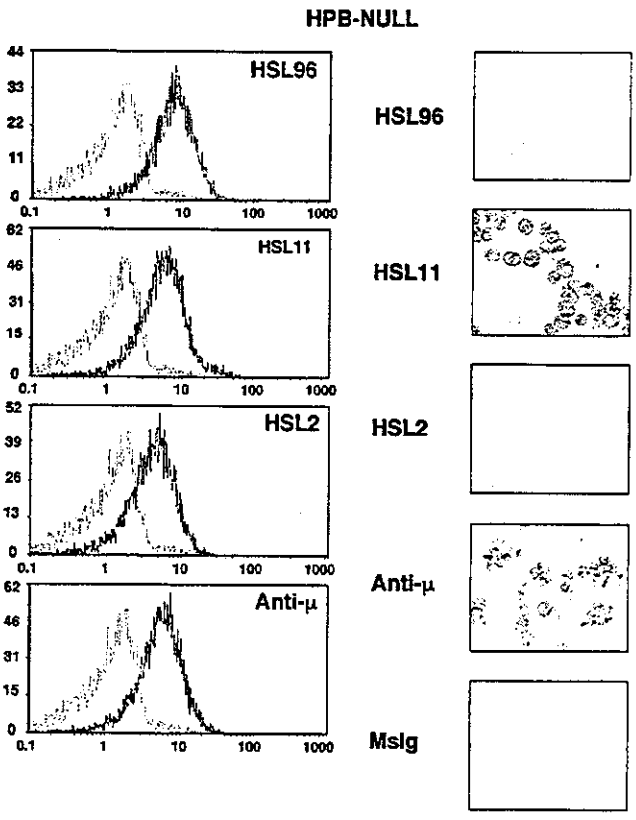

Figure 1 Immunohistochemical detection of CD179b by HSL11 in acetone-fixed, cytocentrifuged precursor B-ALL cell lines. Pre-BCR-expressing HPB-NULL cells were permeabilized and stained with specific mAbs, as indicated, and analyzed using flow cytometry (left panels). The resulting histograms (solid lines) were superimposed on those of the negative control (cells stained with isotype-matched control mouse Ig, broken light lines) and displayed. *X*-axis, fluorescence intensity; *Y*-axis, relative cell number. In parallel, HPB-NULL cells were cytocentrifuged, acetone-fixed, and stained with each mAb, as indicated, using immunohistostaining (right panels). HSL11 is strongly positive and anti-μ is moderately positive, but others are negative. MsIg, iso-type matched control mouse immunoglobulin.

Immunohistochemical Staining of CD179a/b in Acetone-fixed Fresh Frozen Tissues

Next, we used immunohistochemistry to examine whether VpreB8 and HSL11 could detect CD179a/b in clinical childhood B-LBL specimens. When acetone-fixed fresh frozen sections prepared from biopsy specimens obtained from B-LBL patients were examined using immunohistochemical staining, both VpreB8 and HSL11 were found to react with the tissues (Figure 2 and Table 1). Typically, a diffuse cytoplasmic staining pattern was observed in B-LBL tissues using both mAbs (Figure 2). Cases were considered as positive if most of the blasts present in the tissue were clearly stained. As summarized in Table 1, nine out of 10 (90%) B-LBL patients and eight out of 11 (73%) B-LBL patients were positive for VpreB8 and HSL11, respectively. In contrast, no positive staining for VpreB8 or HSL11 was seen in either the Burkitt lymphoma tissues (seven cases) or the diffuse large B-cell lymphoma tissues (three cases), suggesting that both VpreB8 and HSL11 react specifically with B-LBL cells, but not with mature B-cell lymphomas in childhood.

We also examined the other pediatric tumors that must also be included in a differential diagnosis of B-LBL. As presented in Table 2, when acetone-fixed fresh frozen sections prepared from biopsy specimens obtained from seven T-LBL cases, three extramedullary myeloid tumors, and two Ewing sarcoma cases were examined similarly, all of these cases were negative for both VpreB8 and HSL11, indicating the specificity of these mAbs to B-LBL cells.